Bioorganic & Medicinal Chemistry 17 (2009) 2793–2811

Contents lists available at ScienceDirect

Bioorganic & Medicinal Chemistry

journal homepage: www.elsevier.com/locate/bmc

Solution studies on the complex of 4′-epiadriamycin-d-$(CGATCG)_2$ followed by time-resolved fluorescence measurement, diffusion ordered spectroscopy and restrained molecular dynamics simulations

Prashansa Agrawal [a], Sudhir Kumar Barthwal [b], Girjesh Govil [c], Ritu Barthwal [a,*]

[a] Department of Biotechnology, Indian Institute of Technology Roorkee, Roorkee 247 667, India
[b] Department of Physics, Indian Institute of Technology Roorkee, Roorkee 247 667, India
[c] Chemical Physics Group, Tata Institute of Fundamental Research, Homi Bhabha Road, Navy Nagar, Colaba, Mumbai 400 005, India

ARTICLE INFO

Article history:
Received 7 December 2008
Revised 14 February 2009
Accepted 18 February 2009
Available online 24 February 2009

Keywords:
4′-Epiadriamycin-d$(CGATCG)_2$ complex
Nuclear magnetic resonance spectroscopy
Time-resolved fluorescence measurement
Diffusion ordered spectroscopy and restrained molecular dynamics

ABSTRACT

4′-Epiadriamycin is a better-tolerated anthracycline drug, due to lesser cardiotoxicity. We report here a study of the 2:1 complex of 4′-epiadriamycin-d-$(CGATCG)_2$ by proton Nuclear Magnetic Resonance Spectroscopy which show the absence of sequential connectivities between C1pG2 and C5pG6 base pair steps and presence of intermolecular cross peaks of the drug and DNA. Our studies establish the role of 9OH, NH_3^+, 7O, $4OCH_3$ groups in binding to DNA. Time-resolved fluorescence measurement and diffusion ordered spectroscopic studies reveal the formation of complex. The nonspecific interactions as well as those essential for biological activity are discussed along with its medicinal importance.

1. Introduction

The anthracycline family of antibiotics is effective in treating a variety of cancers.[1,2] The therapeutic properties of the various members of the family are attenuated by the chemical substituents on the fused ring system and on the amino sugar.[1,3] Analogs have been synthesized in order to circumvent the adverse toxic effects of these drugs.[4] The 4′-epiadriamycin (Fig. 1a) developed recently is better tolerated due to lesser cardiotoxicity. 4′-Epiadriamycin has been an outcome of the constant search to look for new ligands or modify the existing drugs in order to overcome the adverse effects of cell toxicity or tumor-resistance. It differs from adriamycin only by an inversion of the stereochemistry at the 4′-position of the sugar. The understanding of drug–DNA interaction is the first step to realize potent activity and low toxicity of these drugs.

A wealth of studies has been performed to understand the structural, kinetics, and energetics of interaction[5–9] between the anthracycline drug and DNA. Theoretical studies[10] have suggested that it preferentially recognizes a triplet sequence, with the sequences 5′GCT and 5′CGA being the most energetically favored. DNase I foot printing titration procedure identified the most strongly preferred daunomycin binding site to be the triplet sequences 5′CGA, 5′CGT, 5′CGA and 5′GCT, indicating that either A or T may occupy the position neighboring the intercalation site.[11] The X-ray crystal structure analysis of adriamycin with d-CGATCG[12] has revealed hydrogen bonding of 9OH moiety of drug with G2N1H and G2N3. Further NH_3^+ moiety of daunosamine sugar forms hydrogen bonds with O2 of C5, O4′ of C5, and O2 of T4 residues. The X-ray crystallographic studies on d-TGTACA and d-TGATCA with daunomycin[13] and 4′-epiadriamycin[14,15] have shown sequence dependence of the binding of amino sugar to the A–T base pair outside the intercalation site.

In addition several other van der Waal's contacts also help in stabilizing the complex. Solution structure of adriamycin with d-CGATCG by Nuclear Magnetic Resonance Spectroscopy[16] and molecular modeling studies[17] of daunomycin with d-$(CGCGCGATCGCGCG)_2$ have shown that there exists a conformational equilibrium between different populations of conformers. A *trans* form for backbone torsional angle C3′–O3′–P–O5′, ζ, is observed at G2pT3 and C5pG6 units. Further O-glycosidic bond angle C7′–O7–C1′–C2′-centered around 59° having an energy barrier of 1.4 kcal mol^{-1} from the usual 137° conformer may be present[17] which will change the disposition of NH_3^+ moiety in minor groove of DNA.

The interaction involving intercalation of planar chromophore (ring BCD) of the drug at the 5′pyrimidine–purine 3′ sequence, that is, d-CpG or d-TpG step is found to be preserved due to direct involvement of guanine present at the second position in DNA sequences in binding. The complex is stabilized by two hydrogen

* Corresponding author. Tel.: +91 1332 285807/285484; fax: +91 1332 273560.
E-mail addresses: ritubfbs@iitr.ernet.in, ritubarthwal@yahoo.co.in (R. Barthwal).

0968-0896/$ - see front matter © 2009 Elsevier Ltd. All rights reserved.
doi:10.1016/j.bmc.2009.02.032

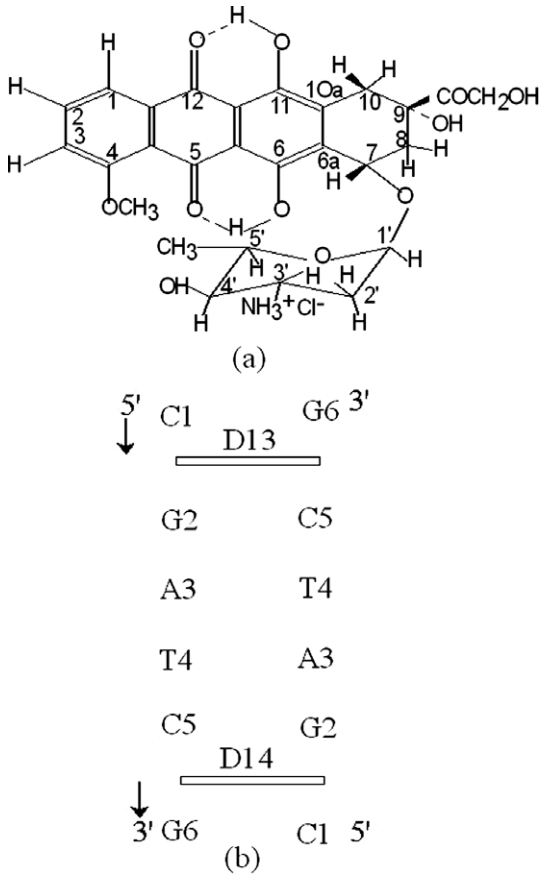

Figure 1. (a) Molecular structure of 4′-epiadriamycin (b) schematic representation of the 2:1 4′-epiadriamycin-d-$(CGATCG)_2$ complex.

bonds, N2H and N3 of guanine with 9O and 9OH of the drug, respectively, in all complexes. The amino sugar lies in the minor groove forming up to five hydrogen bonds with the adjacent intercalating second base, adjacent third base pair and water molecules. The amino group is located closer to the second base pair in 5′–3′ sequence and its sugar edge. This tends to make shorter van der Waal's and hydrogen bond contacts with d-CGATCG than that with d-CGTACG. This demonstrated the role of third base pair, suggested also by theoretical energy calculations.[10] The conformation of the ring A of the drug in complexes with d-TGATCA is H8 with C8 atom deviating 0.71 Å away from sugar. On the other hand, in d-TGTACA, d-CGTACG complexes, ring A conformation is 9H with C9 atom deviating by 0.53 Å and 0.59 Å, respectively, towards daunosamine sugar. The hydroxyl group at C14 position in 4′-epiadriamycin/adriamycin is involved in additional contact through water molecule to the DNA phosphate resulting in further stabilization of the complex. The torsional angle in glycosyl linkage of the daunomycin molecule is significantly reduced from 162–167° to 1272013144° while the daunomycin sugar is in unsymmetrical boat or chair conformation in the various structures of the complexes. Thus both DNA and drug exhibit considerable conformational flexibility in these complexes.

The present study has been done on 4′-epiadriamycin-d-$(CGATCG)_2$ complex using NMR with the aim that NMR has the advantage of providing information about the system in solution and also yields insights into dynamic processes. The existence of bound and free resonances of imino protons of DNA clearly demonstrates that the drug indeed binds to the DNA hexamer and there is a slow exchange of free and bound DNA on NMR time scale at low temperature. Here, we have chosen the self-complementary duplex d-$(CGATCG)_2$ since this contains two symmetrically equivalent CGA and TCG 4′-epiadriamycin binding sites and thus 2:1 4′-epiadriamycin–duplex complex retains the twofold symmetry of the free DNA. Sequence specific assignment of small DNA duplex is well established and that for drug molecule has been taken from our paper.[18] We present here our results on interaction of 4′-epiadriamycin with d-$(CGATCG)_2$ (Fig. 1b). We have reported the ^{1}H NMR results of titrations of drug with DNA followed by change in chemical shift, analysis of NOE data, the drug–DNA contacts and the structural features of drug and DNA hexamer in the complex. The inter-proton distance restraints have been used to carry out molecular dynamics simulations. The final convergent structure has been analyzed with respect to helicoidal parameters and backbone torsional angles. The conformation of ring A and daunosamine sugar has been obtained. Specific intermolecular contacts have been extracted and correlation between different structural parameters has been investigated. We have obtained conformational parameters, correlations between them and intermolecular contacts to establish the mode of binding. Time-resolved fluorescence measurement and diffusion ordered spectroscopic studies[19] have been done to show that there is complex formation. A complete comprehensive view of the drug–DNA interaction with a purpose of understanding molecular basis of action is presented in this manuscript.

2. Results and discussion

2.1. NMR studies on complex of 4′-epiadriamycin-d-$(CGATCG)_2$

The proton NMR spectra of the complex of 4′-epiadriamycin-d-$(CGATCG)_2$ at various drug (D)/DNA (N) ratios, D/N = 0.16, 0.32, 0.48, 0.64, 0.80, 0.96, 1.11, 1.27, 1.43, 1.53, 1.60, 1.75, 1.91 and 2.03 at 275 K are recorded, few are shown in Figure 2a–c. At 275 K, the imino proton signals are sharpened and intensified. Besides, DNA is expected to be present completely in duplex state at 275 K. The assignment of nucleotide protons (Table 1a) are done using the standard strategies, that is, sequential NOEs (base H8/H6)$_n$-sugar (H1′)$_{n-1}$, (base H8/H6)$_n$-sugar(H2″)$_{n-1}$, (base H8/H6)$_n$-sugar(H2′)$_{n-1}$ and drug protons (Table 1b) are assigned using Barthwal et al.[18] as the reference. On addition of 4′-epiadriamycin to d-$(CGATCG)_2$, new drug proton signals are seen which increase in intensity with D/N ratios. This is evident from the resonance signals of 1′H, 7H, 5′CH_3, 6OH, 11OH, 1H, 2H and 3H protons shown in Figure 2a–c. The initially sharp NMR spectral lines of free DNA duplex broaden significantly without the appearance of a new set of NMR resonances for the bound complex. Both the nucleotide and drug protons, each having one set of resonances, shift gradually from their position in uncomplexed state with D/N ratio (Supplementary data 1 and 2). The spectra of the complex of 4′-epiadriamycin-d-$(CGATCG)_2$ as a function of temperature are obtained at D/N = 1.0, 1.5 and 2.0 (Fig. 3a and b) at the range 275–328 K (Supplementary data 3a–c and 4).

2.1.1. Characteristic of drug–DNA complex

In uncomplexed or free d-$(CGATCG)_2$, T4NH and G2NH peaks appear at 13.74 and 12.95 ppm, respectively, while the G6NH resonance is not seen presumably due to exchange with water solvent. On successive addition of 4′-epiadriamycin to DNA, four additional resonance peaks are observed at 11.89, 13.75, 12.16, 12.01 ppm besides the 6OH and 11OH peak at about 13.81 and 12.41 ppm. In 2D NOESY spectra (Fig. 4a) pairs of protons resonating at 12.84, 11.89; 13.69, 13.75 and 12.16, 12.01 give cross peaks (shown in circle) with each other. Since T4NH and G2NH appear at 13.74 and 12.95 ppm in uncomplexed/d-$(CGATCG)_2$, the peaks at 13.75 and 11.89 ppm get assigned to T4NH and G2NH in the com-

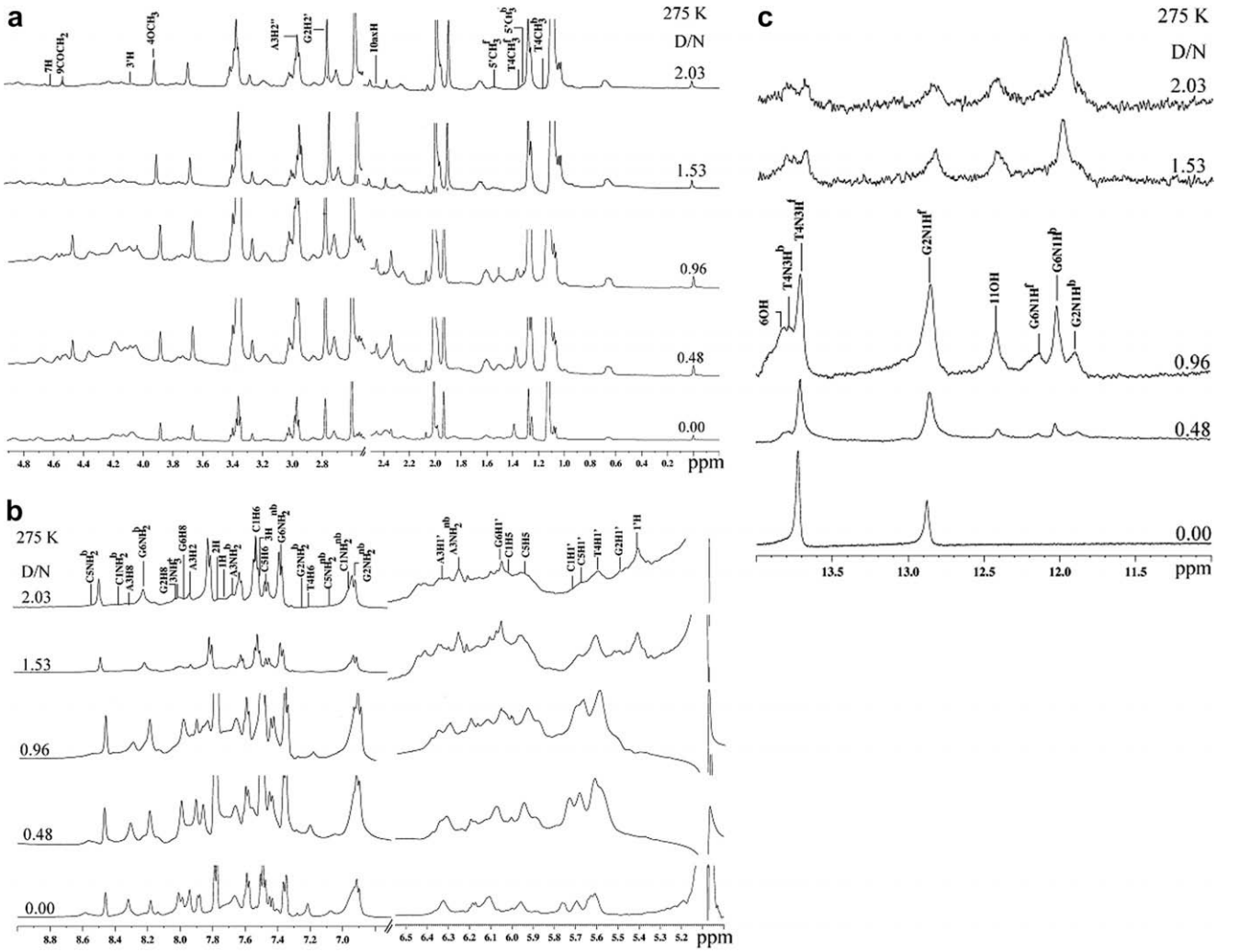

Figure 2. (a–c) Proton NMR spectrum of the complex 4′-epiadriamycin d-$(CGATCG)_2$ complex as a function of added drug (D) to DNA (N) duplex stoichiometric ratios (D/N) of 0.0, 0.48, 0.96, 1.53, 2.03 at 275 K in H_2O/D_2O.

Table 1a
Chemical shift (ppm) of nucleic acid protons in uncomplexed state (δ^f) and that bound to drug (δ^b) at drug (D) to nucleic acid duplex (N) ratio D/N = 1.0 at 275 K

Proton	C1			G2			A3			T4			C5			G6		
	δ^b	δ^f	$\Delta\delta$	δ^b	δ^f	$\Delta\delta$	δ^b	δ^f	$\Delta\delta$	δ^b	δ^f	$\Delta\delta$	δ^b	δ^f	$\Delta\delta$	δ^b	δ^f	$\Delta\delta$
H8/H6	7.51	7.69	−0.18	7.99	8.05	−0.06	8.30	8.34	−0.04	7.19	7.26	−0.07	7.45	7.51	−0.06	7.87	8.02	−0.15
H1′	5.71	5.92	−0.21	5.52	5.62	−0.10	6.31	6.37	−0.06	5.61	5.70	−0.09	5.68	5.72	−0.04	6.06	6.18	−0.12
H2′	1.82	2.02	−0.20	2.74	2.89	−0.15	2.71	2.80	−0.09	2.02	2.09	−0.07	1.95	2.06	−0.11	2.62	2.78	−0.16
H2″	2.34	2.45	−0.11	2.86	2.99	−0.13	2.99	3.08	−0.09	2.42	2.52	−0.10	2.36	2.49	−0.13	2.32	2.42	−0.10
H3′	4.66	4.80	−0.14	4.74	4.82	−0.08	5.05	5.11	−0.06	4.88	4.95	−0.07	4.84	4.91	−0.07	4.68	4.74	−0.06
H4′	4.08	4.11	−0.03	4.36	4.40	−0.04	4.51	4.53	−0.02	4.19	4.22	−0.03	4.15	4.19	−0.04	4.19	4.22	−0.03
H5′	3.78	3.77	+0.01	4.15	4.19	−0.04	4.29	4.32	−0.03	4.08	4.11	−0.03	4.08	4.11	−0.03	4.15	4.19	−0.04
H5″	3.72	3.75	−0.03	4.10	4.16	−0.06	4.19	4.22	−0.03	3.94	4.04	−0.10	3.94	4.04	−0.10	4.10	4.16	−0.06
H5/H2	6.00	6.02	−0.02	*	*	*	7.84	7.92	−0.08	*	*	*	5.93	5.98	−0.05	*	*	*
$NH2^b$	8.31	8.41	−0.10	7.21	7.45	−0.24	7.62	7.78	−0.16	*	*	*	8.52	8.67	−0.15	8.20	8.18	+0.02
$NH2^{nb}$	6.97	6.93	+0.04	6.95	6.91	+0.04	6.12	6.21	−0.09	*	*	*	7.05	7.15	−0.10	7.34	7.36	−0.02
		$^{\#}\delta^b$	$^{\#}\delta^f$	$\Delta\delta^{\#}$		$^{\#}\delta^b$	$^{\#}\delta^f$	$\Delta\delta^{\#}$		$^{\#}\delta^b$	$^{\#}\delta^f$	$\Delta\delta^{\#}$						
CH_3	*	*	*	*	*	*	*	*	*	1.20	1.37	−0.17	*	*	*	*	*	*
NH	*	*	*	11.89	12.84	−0.95	*	*	*	13.75	13.69	+0.06	*	*	*	12.01	12.16	−0.15

−ve $\Delta\delta$ indicates upfield shift.
+ve $\Delta\delta$ indicates downfield shift.
Also shown here is the change in chemical shift on binding, that is, $\Delta\delta = \delta^b{}_{(D/N=1.0)} - \delta^f$ and $\Delta\delta^{\#} = {}^{\#}\delta^b - {}^{\#}\delta^f$.

plex of d-$(CGATCG)_2$ with drug at D/N = 2.0 (designated as $T4NH^b$ and $G2NH^b$). The remaining pair (12.16, 12.01 ppm), gets assigned to G6NH present in free ($G6NH^f$ 12.16 ppm) and bound state ($G6NH^b$ 12.01 ppm). The area under the NH peaks, confirmed that the G2NH/T4NH/G6NH indeed split into two sets of peaks. The ratio of area of $T4NH^f$ to $T4NH^b$ decreased from 3:1 (approximately)

Table 1b
Chemical shift (ppm) of drug protons in uncomplexed monomer a state ($\delta^{monomer}$ concentration 0.01 mM, 298 K), free (δ^{f}, 8.0 mM, 275 K) and that bound (δ^{b}) to nucleic acid duplex at drug (D) to DNA (N) ratio, D/N = 1.0 at 275 K

Protons	δ^{b} (D/N = 1)	δ^{f}	$\Delta\delta = \delta^{b}(D/N = 1) - \delta^{f}$	$\delta^{monomer}$	$\Delta\delta' = \delta^{b}(D/N = 1) - \delta^{monomer}$
1H	7.66	7.11	+0.55	7.81	−0.15
2H	7.73	7.35	+0.38	7.85	−0.12
3H	7.49	7.08	+0.41	7.55	−0.06
7H	4.72	4.51	+0.21	4.60	+0.12
1′H	5.39	5.22	+0.17	5.46	−0.07
3′H	4.07	3.25	+0.82	3.31	+0.76
4′H	4.18	3.22	+0.96	3.13	+1.05
5′H	4.27	3.84	+0.43	4.01	+0.26
5′CH_3	1.31	1.22	+0.09	1.33	−0.02
4OCH_3	3.91	3.64	+0.27	3.95	−0.04
9O$COCH_2$	4.49	4.66	−0.17	4.86	−0.37
6OH	13.81	12.96	+0.85	—	—
11OH	12.41	12.31	+0.10	—	—
9OH	5.08	4.96	+0.12	—	—
3NH_3^+	7.95	8.00	−0.05	—	—
4′OH	4.82	4.91	−0.09	—	—
8eqH	2.36	2.07	+0.29	2.18	+0.18
8axH	1.82	1.79	+0.03	2.13	−0.31
2′axH	1.82	1.76	+0.06	1.87	−0.05
2′eqH	2.34	2.11	+0.23	2.31	+0.03
10eqH	2.64	2.67	−0.03	3.10	−0.46
10axH	2.38	2.20	+0.18	2.92	−0.54

−ve $\Delta\delta$ indicates upfield shift.
+ve $\Delta\delta$ indicates downfield shift.
Also shown here is the change in chemical shift, due to binding, that is, $\Delta\delta = \delta^{b}(D/N = 1) - \delta^{f}$ and $\Delta\delta' = \delta^{b}(D/N = 1) - \delta^{monomer}$.

at D/N ratio of 1.0 to 2:1 at D/N ratio of 2.0, that is, on addition of an increasing amount of drug to DNA. It is noted that the intensity of G6NH^{f} peaks is significantly lesser than that of G2NH^{f} and T4NH^{f}. Also the NOE cross peak of G6NH^{f} and G2NH^{f} resonance corresponding to a distance of 3.72 Å in standard B-DNA structures is weaker in intensity than the NOE cross peak of T4NH^{f} and G2NH^{f} which also corresponds to a distance of 3.72 Å. This suggests that G6NH proton which completely exchanges with water in free d-$(CGATCG)_2$, is immobilized in the drug–DNA complex although it is still fraying to some extent being the terminal base pair of DNA. Accordingly the line width of G6NH^{b} is found to be greater than that of G2NH^{b} and T4NH^{b}.

It is observed that the sharp T4CH_3 peak appearing at 1.37 ppm in d-$(CGATCG)_2$ decreases in intensity as D/N ratio increases and one new, relatively broad peak appearing at 1.20 ppm, respectively, start growing in intensity with D/N (Fig. 2a); the same is also manifestes in the area plot. These peaks exchange with each other and hence the peak at 1.20 ppm gets assigned to T4CH_3 of DNA bound to the drug molecule (T4$CH_3{}^{b}$). The existence of two sets of T4NH, G6NH, G2NH, and T4CH_3 clearly demonstrates that the drug indeed binds to the DNA hexamer and there is a slow exchange of free and bound DNA on NMR time scale at 275 K.

2.1.2. Change in chemical shift due to complexation

There are two intercalative sites available for the drug. The change in chemical shift ($\Delta\delta$) of base and H1′ protons with ratios are gradual and small in magnitude. The $\Delta\delta$ increases with D/N ratio as more of hexamer binds to the drug and a maximum of 0.20 ppm upfield shift is observed for C1H1′ and G2H1′ protons. T4NH bound imino proton is downfield shifted with respect to the corresponding imino protons in free state; the shift being 0.06 ppm, whereas G2NH and G6NH bound imino protons are upfield shifted and the shifts are 0.95 and 0.15 ppm, respectively (Table 1a, Fig. 4a, cross peaks are encircled). Such changes may be attributed to stacking or structural changes in complexation. ^{1}H resonance signals are observed on addition of increasing amount of drug in the temperature range 275–328 K at steps of 5 K (Supplementary data 3a–c, Fig. 3a and b). Till 308 K temperature, the signals are in slow exchange regime and are sufficiently broad to be followed individually through the titration. It is observed that there is variation of chemical shift with temperature showing downfield shift of 0.25 ppm for C1H1′ and 0.28 ppm for C5H1′ at D/N 2.0. There is noticeable change in the drug and nucleic acid protons in the range 275–328 K. This indicates that structurally only one complex is being formed and the chemical shift at any one temperature is not an average of bound and unbound DNA/drug, the equilibrium of which is likely to shift with temperature. The area plots of T4NH, G2NH, G6NH and T4CH_3 in bound and free state also confirm that only one bound species exists in this temperature range. The gradual change with temperature in the range 275–328 K may be due to destacking/decreased intercalation and duplex to single strand transition.

2.1.3. Chemical shift of 4′-epiadriamycin in the drug–DNA complex

There is a gradual shift in drug protons on binding to DNA. The ring protons, 1H, 2H and 3H, shift upfield substantially up to 0.6 ppm with respect to the chemical shift position of drug monomer, $\delta^{monomer}$ in 2:1 drug to DNA complex at 275 K (Supplementary data 2). The downfield shift $\Delta\delta = \delta^{b} - \delta^{f}$ is 0.40 ppm for 3H, 0.37 ppm for 2H, 0.56 ppm for 1H, 0.23 ppm for 1′H proton and 0.85 ppm for 6OH at 275 K (Supplementary data 2). Several protons in ring A and D of the drug experience large upfield shifts, up to 0.55 ppm. It is worth noting that there is downfield shift up to 0.96 and 0.82 ppm for 4′H and 3′H, respectively. This is due to inversion of 4′H and 4′OH in 4′-epiadriamycin in comparison to adriamycin in which these shifts are 0.29 and 0.19 ppm, respectively. This may be due to better stacking of 4′-epiadriamycin with DNA. The maximum change in chemical shift with temperature is observed for 6OH, 11OH, 1H, 2H, 3H and 1′H protons (Supplementary data 4), which are presumably close to oligomer due to stacking of 4′-epiadriamycin chromophore with base pair of DNA. These have been attributed to intercalation of drug chromophore between base pairs of DNA, which move apart to a distance of ~6.8 Å on binding to drug[14,15] and are characteristic of stacking interaction between aromatic/conjugated rings. The relatively

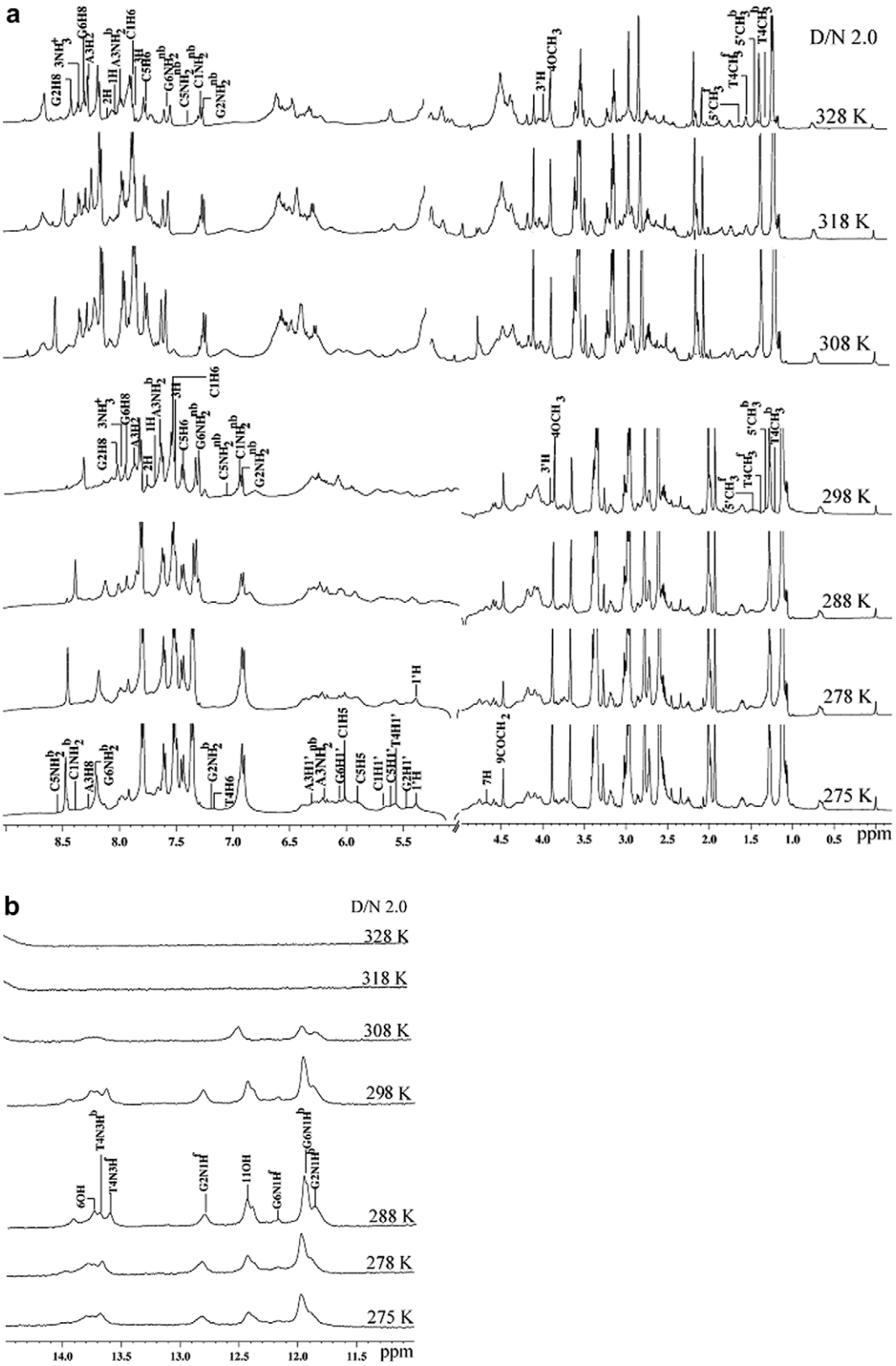

Figure 3. (a, b) Proton NMR spectrum of the complex 4′-epiadriamycin d-$(CGATCG)_2$ complex as a function of temperature (275–328 K) at drug (D) to DNA (N) duplex stoichiometric ratios (D/N) of 2.0 in H_2O/D_2O.

smaller change in 1H and 2H protons of drug, also reported earlier,[20–22] may be due to specific positioning of drug chromophore between base pairs such that the ring A partially protrudes out of base pairs resulting in much lesser overlap with adjacent base pairs and hence experiencing less ring current shifts. The base pair protons (H8, H6, H2, H5, CH_3) and deoxyribose H1′ protons (being close to aromatic ring) of the intercalating base pair of DNA show ring current effect to a much lesser extent since they are destacked

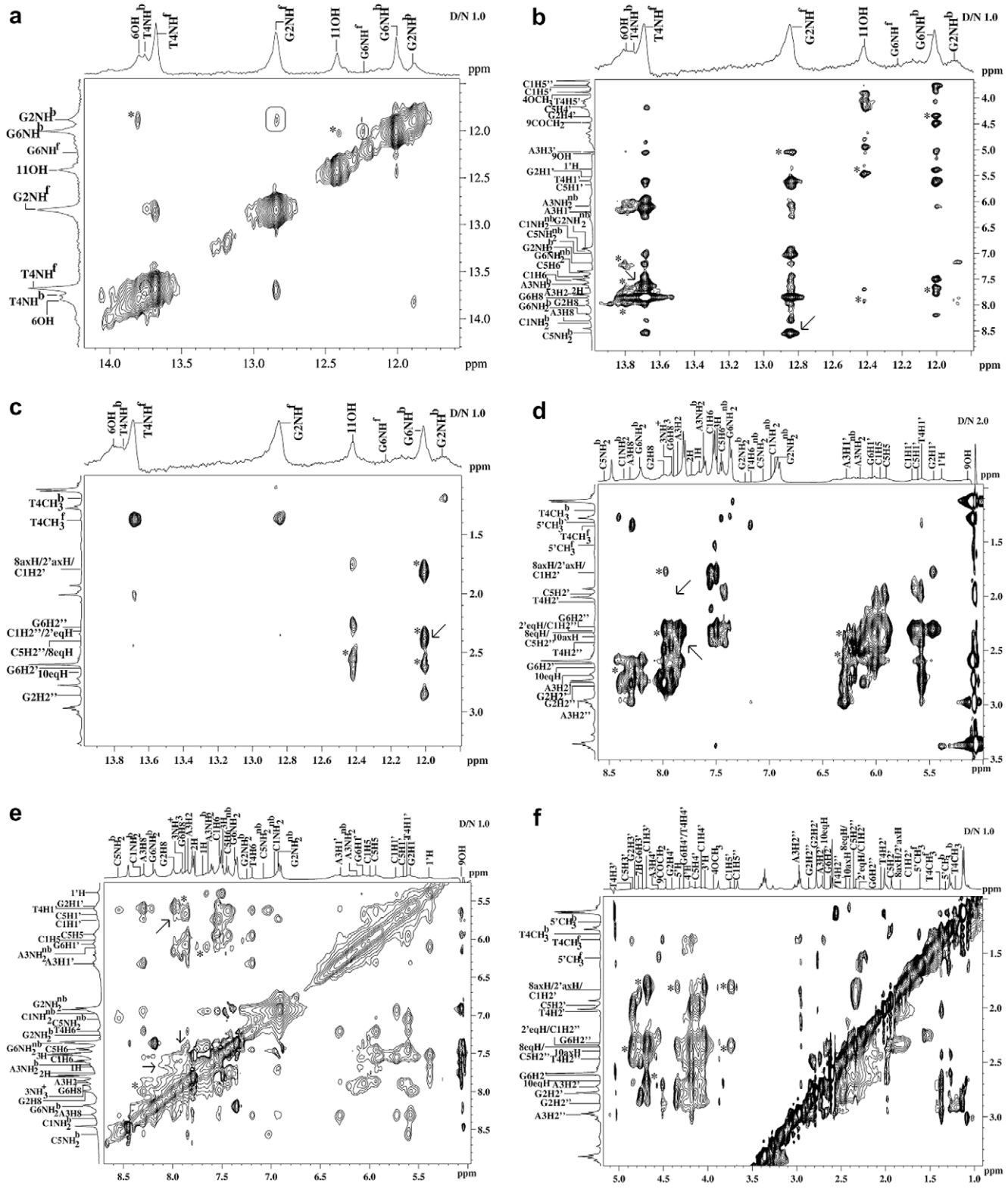

Figure 4. (a–f) Expansions of various regions of 2D NOESY spectrum of 4′-epiadriamycin-d-(CGATCG)$_2$ complex in H_2O/D_2O and intermolecular cross peaks are shown by asterisk (*) between drug and DNA and (→) indicate loss of connectivity between base pair step at 275 K.

from the neighboring base pair in free DNA and then stacked with the conjugated aromatic rings ABCD (Fig. 1a) of 4′-epiadriamycin. The observed chemical shift at different temperatures (Fig. 3a and b) is distinctly different from that of free drug in monomer/self associated form[21,22] or free DNA.[23] These changes in chemical shift may be due to structural alterations on binding and cannot be correlated directly to a specific structural parameter; hence not a sufficient marker of interaction. Therefore 2D NOESY data are acquired which gives inter-proton contacts and shows that the major conformer is the 2:1 molecular complex.

2.1.4. Conformational features of DNA and drug in the complex

The NOESY spectra of drug–DNA complex at stoichiometric D/N ratio of 1.0 have been investigated extensively at mixing time (τ_m) of 100, 200 and 300 ms. The inter-proton distances have also been evaluated by taking distance CH5–CH6 = 2.45 Å for τ_m = 200 ms as an internal standard. The observed NOEs for (a) connectivities involving amino and imino protons of base pairs, (b) sequential connectivities (c) intranucleotide connectivities within sugar (d) intranucleotide base to sugar connectivities are given in Supplementary data 5–7 and Table 2.

2.1.4.1. Connectivities involving amino and imino protons of base pairs. The base sequence d-$(CGATCG)_2$ being self-complementary is responsible for a high symmetry in the NMR spectra. The observation of NOEs (Fig. 4a–c, shown by arrow) between the C1H2″–G6N1H^b; G2N1H^f–C5N4H2^b; A3H2–T4NH^b; T4NH^b–A3N6H2^b establish Watson–Crick base pairing between T1···A6, G2···C5 and A3···T4 base pairs in the duplex showing that drug is stabilizing the duplex (Supplementary data 7). The sequential connectivities among adjacent base pairs, at the terminal ends where the binding site is present, are not observed (Table 2). This clearly demonstrates that DNA duplex is intact; apparently sequential connectivities are broken between base pairs to accommodate drug chromophore as expected on binding of typical intercalator to DNA molecule.

2.1.4.2. Sequential connectivities. The results in Table 2 clearly demonstrate a discontinuity in the $(H6/H8)_n$ to $(H1')_{n-1}$, $(H2')_{n-1}$, $(H2'')_{n-1}$, $(H3')_{n-1}$, base $(H6/H8)_{n-1}$ sequential NOE connectivities expected in right-handed B-DNA geometries at the C1pG2 and C5pG6 steps (Fig. 4d and e and Supplementary data 8 and 9, shown by arrow) by the intercalation of anthracycline ring of the drug. Intense NOE cross peaks are observed for several sequential connectivities between the steps, G2pA3, A3pT4 and T4pC5, as expected for right handed B-DNA type conformations. The intensities corresponding to these sequential NOE connectivities, $(H1', H2', H2'')_{n-1}$–(base H8/H6)$_n$ are found to be in the range 2.3–4.0 Å (Table 2). Thus the drug chromophore intercalates at C1pG2 and C5pG6 steps. The cross peaks A3H8–G2H8 (5.0 Å), A3H8–T4CH$_3$ (3.8 Å), A3H8–T4H6 (4.8 Å) and T4H6–C5H5 (3.9 Å) have earlier been observed in the spectra of d-$(CGATCG)_2$[23] and d-$(TGATCA)_2$.[24] These observations are indicative of good base to base stacking at these base pair steps. The stacking pattern in the base pairs adjacent to the intercalation site appears to have changed on complexation.

Table 2
Some of the inter residue sequential NOE cross peaks (ds) of nucleotide protons in the drug–DNA complex observed in NOESY spectra (Fig. 4a–f and Supplementary data 8 and 9) of drug–DNA complex at D/N = 1.0, 1.5 and 2.0 at 275 K

Inter-residues sequential peaks	D/N = 1.0	D/N = 1.5	D/N = 2.0
G2H8–C1H1′	—	—	—
G2H8–C1H2′/2′axH/8axH	o	o	o
G2H8–C1H2″/2′eqH	o	o	o
G2H8–C1H6	—	—	—
G2H1′–C1H6	—	—	—
G2H8–C1H3′	w	w	—
A3H8–G2H1′	s	s	ws
A3H8–G2H2′	ws	ws	w
A3H8–G2H2″	w	w	ww
A3H8–G2H8	s	s	w
T4H6–A3H1′	s	s	ww
T4H6–A3H2′	w	w	w
T4H6–A3H2″	ws	w	ww
T4H1′–A3H8	s	s	s
T4CH$_3$–A3H8	ss	ss	s
T4H6–A3H8	s	s	w
C5H6–T4H1′	ss	s	w
C5H6–T4H2″	s	s	w
C5H6–T4H2′	ss	ss	w
C5H6–T4H3′	s	ss	s
C5H5–T4H6	ws	ws	ww
C5H5–T4CH$_3$	s	s	w
G6H8–C5H1′	w	w	—
G6H8–C5H2″/8eqH	o	o	o
G6H8–C5H2′	w	ww	—
G6H8–C5H3′	w	ww	—
G6H8–C5H6	ww	—	—
G6H1′–C5H6	ww	—	—

The very strong (ss), strong (s), medium (ws), weak (w), very weakly (ww) intense cross peaks correspond to distances in the range ss 1.8–2.5 Å, s 2.5–3.0 Å, ws 3.0–3.5 Å, w 3.5–4.0 Å, ww 4.0–5.0 Å, respectively. Overlap of cross peaks is indicated as o.

2.1.4.3. Intranucleotide connectivities within sugar. Sugar conformation may be determined from the integrals of cross peaks in NOESY spectra (Supplementary data 5) at 275 K. Intra residue inter-proton distances H1′–H4′ and H2″–H4′ distances vary significantly with P_S and χ_S, respectively, hence may be used for conformational analysis. The NOE connectivity corresponding to H1′–H4′ for G2 residue is weakly intense as compared to A3 and G6 residues (Supplementary data 5). This indicates that pseudo rotation phase angle for G2 residue is ~162°. The observed distance from H1′–H4′ NOE intensity (Supplementary data 5) increases in the order G6 < A3 < G2 and T4, C1, C5 are overlapped, hence cannot be resolved at τ_m = 200 ms. Thus the pseudorotation P_S decreases as G2 > A3 > G6 so that the P_S of G6 residue is estimated as <144°. The distance H2″–H4′ decreases rapidly from 3.8 Å for P_S = 162° to 2.3 Å for P_S = 18° while its variation with P_S in the range P_S = 144–180° is negligible.[25] The observed values of H2″–H4″ distance (Supplementary data 5) show that G2, A3 and G6 have distance ~3.8 Å, hence the fraction of N-conformer is very less in the residues. All other observed intra-sugar NOE intensities (e.g., relatively higher value of H2″–H3′ and H3′–H4′ distance for G2 residue) are in agreement with these estimations of P_S and χ_S and also indicate that G2 residue is closest to the B-DNA conformation. The observed intense cross peaks corresponding to H2″–H3′ and H3′–H4′ distances show that the S-conformer is predominant.

2.1.4.4. Intranucleotide base to sugar connectivities. Among purines, H8–H1′ distance increases in the following order: G2 < G6 < A3 (Supplementary data 6), which shows χ value of G2 residue is close to ~105°. Among pyrimidines, H6–H1′ distance increases as C1 < C5 < T4 indicating that χ value of C1 is close to ~150° (Supplementary data 9, Fig. 4e and f). The H8/H6–H2″ NOE cross peaks show that the distance is least in G2 and C1 residues among the purines and pyrimidines, respectively, and thus these two residues may be adopting high anti conformation. The distance increases in the order G2 < G6 < A3 and C1 < C5 < T4 among purines and pyrimidines, respectively. Strong H8/H6–H3′ NOE connectivities indicate presence of mixed S and N-conformers in all the residues. Similarly intense cross peaks of base to H4′, H5′, H5″ protons for several residues indicate presence of N-conformer along with major S-conformer in deoxyribose.

2.1.5. Conformation of 4′-epiadriamycin

The intramolecular NOE connectivities within the drug molecule in the drug–DNA complex give information about the conformation of drug (Supplementary data 10). It is observed that the 7H proton is nearly equidistant to 8axH and 8eqH atoms, but since the peaks are overlapped, their distance could not be accurately measured. In daunosamine sugar, the 1′H–4′H and 1′H–5′H distances are lesser than the corresponding distance in the free drug (3.1–4.2 Å). Thus the conformation of ring A as well as daunosamine sugar has changed due to binding. As a result the relative orientation of ring A protons with sugar protons is affected. The distance of 7H

to 1′H and 3′H have increased and corresponding NOE connectivity is not observed. The distance of a $9COCH_2$ proton from 1′H and 3′H proton has increased (no cross peak observed). Apparently, $9COCH_2$ has moved apart from daunosamine sugar moiety. Such changes are different from the one which have been observed in X-ray crystal structure of complexes of daunomycin with d-(TGATCA)$_2$.[13] It has been shown that conformation of ring A changes so that 9OH lies in close proximity to G2N2H and G2N3 atoms in order to form two hydrogen bonds. No such studies have been carried out for 4′-epiadriamycin in solution state by NMR techniques.

2.1.6. Intermolecular interactions

Several intermolecular contacts have been observed in the NOESY spectra (shown with asterisk in Fig. 4a–f and Supplementary data 8 and 9) of major conformer and are listed in Table 3.

Table 3
Relative intensities of intermolecular NOE connectivities between d-(CGATCG)$_2$ and 4′-epiadriamycin molecule in the drug–DNA complex at drug to DNA ratio D/N = 1.0, 1.5 and 2.0 from NOESY spectra (Fig. 4a–f and Supplementary data 8 and 9) at 275 K

S. No.	Intermolecular cross peak	D/N 1.0	D/N 1.5	D/N 2.0
1	A3H8–5′CH_3^b	ww	ww	ww
2	A3H1′–5′CH_3^b	ww	ww	ww
3	T4H1′–5′CH_3^b	ww	ww	ww
4	G2H8–10axH	ww	ww	ww
5	C1H6–10axH	ww	ww	ww
6	G6H1′–10axH	w	w	w
7	G6H1′–10eqH	w	w	w
8	A3H8–3′H	ww	ww	ww
9	G6NH2^b–9$COCH_2$	ws	ws	ws
10	A3H8–5′H	ww	ww	ww
11	G2NH2^{nb}–9$COCH_2$	ws	ws	ws
12	C1NH2^b–9OH	ws	w	w
13	G6NH2^b–9OH	ws	ws	w
14	G6H8–9OH	w	w	w
15	G2H8–9OH	ws	ws	w
16	G6NH2^{nb}–9OH	ww	ww	ww
17	C1H5″/C1H5′–1′H	w	ww	ww
18	G2H4′–1′H	ww	w	w
19	A3NH2^{nb}–1′H	w	ws	ws
20	G6H1′–9OH	ww	ww	ww
21	C1H6–1′H	w	w	ww
22	G6H1′–1H	w	ww	ww
23	A3H8–3NH_3^+	w	ww	—
24	T4H1′–3NH_3^+	w	ww	ww
25	G6H3′–10eqH	w	w	w
26	G2H4′–10axH	w	w	w
27	G2H4′–2′axH/8axH/C1H2′	o	o	o
28	C1H5″/C1H5′–10axH	s	ws	w
29	G6H3′–2′axH/8axH/C1H2′	o	o	o
30	G2N1H^b–6OH	ws	ww	ww
31	G6N1H^b–11OH	ww	ww	ww
32	G6H1′–6OH	ws	w	—
33	G6H2′–11OH	ww	ww	—
34	C1H4′/C5H5′/T4H5′–11OH	ww	ww	—
35	G2H5′/G6H5′/C5H4′–11OH	ww	ww	—
36	G6N1H^b–2′axH/8axH/C1H2′	o	o	o
37	G6N1H^b–C5H2″/8eqH	ww	ww	ww
38	G6N1H^b-10eqH	ww	—	—
39	G6N1H^b–9$COCH_2$	ww	ww	ww
40	C5H3′–3H	ww	ww	w
41	A3H2–5′H	ww	—	—
42	C1H2″/2′eqH–3NH_3^+	o	o	o
43	G2H1′–2′axH/8axH/C1H2′	o	o	o
44	G2H4′–9OH	ww	ww	ww
45	G2H1′–9$COCH_2$	ww	—	—
46	G2NH2^b–6OH	ws	w	—
47	G6H8–6OH	ws	w	ww
48	G2H1′–11OH	ww	ww	ww
49	G2H8–11OH	ws	—	—

The very strong (ss), strong (s), medium (ws) and weakly (w) intense cross peaks correspond to distance of ss 1.8–2.5 Å, s 2.5–3.0 Å, ws 3.0–3.5 Å, w 3.5–4.0 Å, ww 4–5 Å. Overlap of peaks is indicated as o and '—' indicates absence of peak due to broadening.

The existence of NOESY cross peaks C1H6–1H, C1H6–2H, C1H6–3H, G6H1′–1H, C5H6–3H, C1NH2^b–9OH, C5H6–1H, C5H6–2H, G6H1′–6OH (intense NOE cross peak) and G6H2′–11OH (weakly intense cross peak) indicates that the drug chromophore stacks with C1 and C5 residues. Since the $4OCH_3$ proton is closer to C5H6 and C5H5 protons while 1H, 2H, 3H protons are close to C1H6 protons, the drug chromophore is oriented in a direction perpendicular to the long axis of C1.G6 and G2.C5 base pairs. As a result of stacking interactions, the 1′H atom of drug comes in close proximity of G6H1′ and G6H2′ atoms. The daunosamine sugar is in close proximity of third base pair as $5'CH_3$ shows NOE cross peaks with protons of A3 residue. We have selected some intermolecular NOE connectivities discussed above and also the intramolecular NOE connectivities within the drug and within the DNA molecule to build a model of drug–DNA complex. The structure obtained after restrained energy minimization followed by restrained molecular dynamics for 100 ps is shown in Figure 5. It is observed that some of the NOEs observed between overlapping resonant peaks are possible as their corresponding distance in rMD structure is within 4.5 Å. The structure derived by rMD simulations is indeed defined by experimental NOE restraints. The comparison of the distance obtained by NMR and rMD is given in Table 4. This geometry would lead to upfield shifts in ring D and ring A protons due to anisotropic ring current effects from the adjacent base pairs. This is consistent with the observed downfield shifts of 0.03–0.21 ppm in 1′H, 7H, 10axH and 8axH protons. Ring A is seen to protrude out, somewhat towards the solvent and is consistent with the observed downfield shifts in 1H, 2H and 3H protons, being ~0.6 ppm. On accommodating the aromatic chromophore of drug between adjacent base pairs, the overlap geometry is considerably altered leading to shifts in their resonance positions. The base pairs however are well stacked as demonstrated by appearance of NOE cross peaks A3H8–T4CH_3 and T4H1–C5H5.

We have derived the values of pseudorotation phase and glycosidic bond rotation in the rMD structure (Table 5a and b) and compared them with that obtained earlier in similar X-ray crystallographic structures.[12,16,21] There are no such studies on binding of 4′epiadriamycin to d-(CGATCG)$_2$ hexamer sequence by NMR techniques. Table 5a shows that T4 and A3 residues have pseudorotation phase angle of 126° and 107°, respectively. Similar values in the range 121–151° have been observed in complex of daunomycin and 4′-epiadriamycin with d-(TGATCA)$_2$[13–15] for T1, A3 and T4 residues. It may be noted that our NMR results indicate that deoxyribose sugar is a mixture of S- and N-conformers in dynamic equilibrium. The S-conformer exists as the predominant form having pseudorotation P_S in the range 135–162°. Thus these results show the feasibility and relevance of NMR studies of 4′-epiadriamycin bound to d-(CGATCG)$_2$. Some of the features such as NOE connectivities A3H1′–5′CH_3 and G6H1′/A6H1′–1′H are common to complexes with d-(CGATCG)$_2$. But various other detailed structural features appear to be unique to the drug–DNA complex studied. This reflects on drug-specific or DNA sequence specific interactions at molecular level and is relevant to differences in molecular basis of their action.

2.2. TCSPC analysis: time-resolved fluorescence measurements

From TCSPC analysis, it is seen that the fluorescence decay curve profile of free drug is expected to be monoexponential[26,27] but it is biexponential with two lifetimes and two amplitudes. The lifetime of free 4′-epiadriamycin is found to be $\tau_1 = 0.83$ ns, $\tau_2 = 2.19$ and amplitude is $B_1 = 0.06$, $B_2 = 0.03$. This shows that there may be presence of two conformers of the drug or the aggregation of the drug molecule. On the formation of d-(CGATCG)$_2$–4′-epiadriamycin 2:1 complex, $\tau_1' = 0.71$ ns, $\tau_2' = 1.08$ ns; $B_1' = 0.01$ and $B_2' = 0.08$. In the present study the smaller B_1' and higher B_1

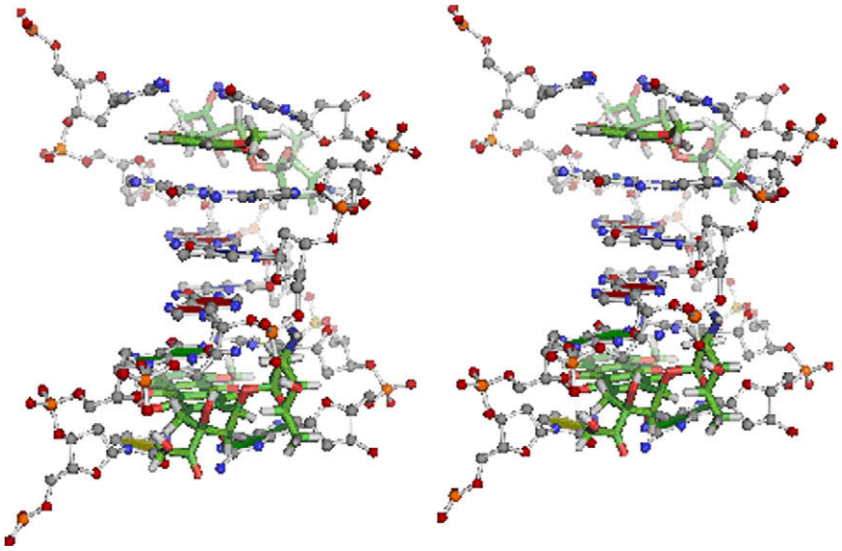

Figure 5. The stereoview of final rMD structure of 4′-epiadriamycin-d-(CGATCG)$_2$ derived from the NOE data.

Table 4
Inter-proton distances (Å) obtained from intermolecular NOE connectivities between hexanucleotide and the drug molecule in the drug–DNA complex from NOESY spectra (Fig. 4a–f and Supplementary data 8 and 9) at 275 K (distances are taken for rMD model from intramolecular and intermolecular peaks of drug and DNA)

S. No.	Intermolecular cross peak	Distance obtained from rMD	
		Experimental distance (Å)	Observed distance (Å)
1	G2H8–10axH	4.34	4.36
2	G6NH2^{nb}–9OH	4.96	4.94
3	G2H4′–10axH	3.74	3.75
4	G2N1H^{b}–6OH	3.59	3.61
5	G6N1H^{b}–11OH	4.44	4.43
6	G6H1′–6OH	3.08	3.06
7	G6N1H^{b}–5H2″/8eqH	4.87	4.88
8	G6N1H^{b}–10eqH	4.98	5.00
9	G2H1′–9COCH$_2$	4.26	4.27
10	G2NH2^{b}–6OH	3.32	3.70
11	G6H8-6OH	3.86	3.86
12	G2H1′–11OH	4.73	4.74
13	G2H8–11OH	3.33	3.35

Table 5a
Comparison of deoxyribose conformation (pseudorotation°)

	Present work		CGA + mor[a]	CGA + adm[b]
	NMR	rMD		
C1	High anti	−150	180	–	148
G2	Anti	−105	−108	−131, −92	−90
A3	Anti	−105 to −120	−136	−148, −146	−130
T4	Anti	−105 to −120	−118	−141, −123	−113
C5	High anti	−90	−86	−105, −112	−90
G6	High anti	−90	−82	−104, −110	−90

[a] CGATCG + morpholinodoxorubicin.[16]
[b] CGATCG + adriamycin.[12]

lifetime components represent the intercalated and free form of the drug, respectively. The τ_1 value ($\tau_1' = 0.71$ ns) of the complex is less than that of τ value ($\tau_1 = 0.83$ ns) of free 4′-epiadriamycin, showing that there is shortening of the decay time of 4′-epiadriamycin due to intercalation (Fig. 6). This indicates the complexation of the DNA base with the drug and is due to electron transfer from the d-(CGATCG)$_2$ to 4′-epiadriamycin. The $\tau_2' = 1.08$ ns component may reflect the other conformations of unprivileged structures. Thus there is clear indication that 4′-epiadriamycin is intercalating in the d-(CGATCG)$_2$ hexamer sequence and forming the complex.

2.3. Diffusion ordered spectroscopy (DOSY) studies on 4′-epiadriamycin-d-(CGATCG)$_2$ complex

DOSY spectra of 4′-epiadriamycin-d-(CGATCG)$_2$ complex of 2:1 D/N ratio is compared with that of 4′-epiadriamycin and d-(CGATCG)$_2$ alone at 275 (Fig. 7a) and 298 K (Fig. 7b). The calculation of diffusion coefficient was done using resonances, which got affected on interaction of drug with DNA. Hence 1H, 2H, 3H of drug and C1H6, G2H8 of DNA resonances had been taken into account. On complex formation, the diffusion coefficient value of the drug resonances in the complex decreases in comparison to that in the uncomplexed drug. The corresponding values of the drug resonances in complex and the drug alone are $0.27 \pm 0.02 \times 10^{11}$ and $1.84 \pm 0.05 \times 10^{-11}$ m^2/s, respectively, and that of d-(CGATCG)$_2$ in the complex and alone hexamer are $2.61 \pm 0.04 \times 10^{-10}$ and $6.30 \pm 0.08 \times 10^{-10}$ m^2/s, respectively, at 275 K. This is due to the interaction of the drug with DNA which slower the rate of diffusion. However, at 298 K, the diffusion coefficient value for the same hexamer signal for complexed and uncomplexed DNA are $2.25 \pm 0.01 \times 10^{-10}$ and $1.38 \pm 0.04 \times 10^{-10}$ m^2/s, respectively, while that for bound and free drug resonance, the values are $5.11 \pm 0.03 \times 10^{-10}$ and $1.53 \pm 0.07 \times 10^{-10}$ m^2/s, respectively. The diffusion coefficient values have been increased on comparing the complexed and the uncomplexed form. This may be due to the fact that the drug starts uncomplexing with increase in temperature. One set of peak is due to averaging of the diffusion coefficients. The exchange is slower at 275 K in comparison to that obtained at 298 K on the diffusion time scale.

2.4. Restrained molecular dynamics studies

The nucleotides are labeled from C1 base paired to G12 with C1 to G6 in the 5′ to 3′ direction on strand 1 and from C7 to G12 on strand 2. The 4′-epiadriamycin molecules are numbered D13 and D14 and the atomic numbering scheme for the molecule is shown in Figure 1a and schematic representation of drug–DNA complex is shown in Figure 1b. The various superimposed structures obtained by restrained molecular dynamics simulations are shown in Figure 8. The drug–DNA complex is stabilized via close contacts, which in-

Table 5b
Comaprison of glycosidic bond rotation (°)

	Present work		CGA + mor[a]	CGA + adm[b]	CGA + dnm[c]	CpG + dnm[d]
	NMR	rMD				
C1	153–162	−139	120, 143	158	160	153
G2	180	130	95, 136	141	142	135
A3	153–162	107	77, 73	129	131	
T4	144	126	92, 130	124	122	
C5	153–162	143	137, 119	151	141	
G6	162	185	147, 142	161	165	

CGATCG + morpholinodoxorubicin[16]; bCGATCG + adriamycin.[12]
[a] CGATCG + morpholinodoxorubicin.[16]
[b] CGATCG + adriamycin.[12]
[c] CGATCG + daunomycin.[12]
[d] CpG + daunomycin.[21]

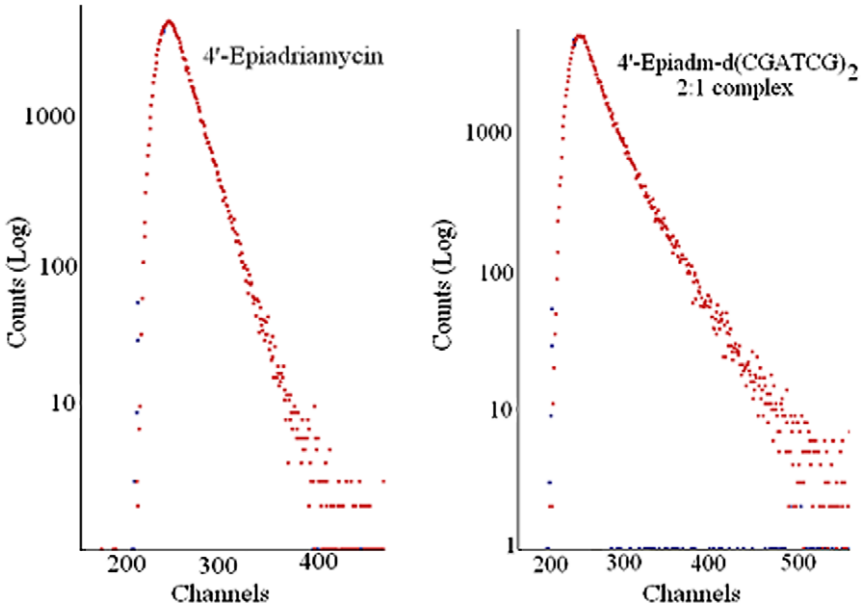

Figure 6. Fluorescence lifetime decay measurement profile of 4′-epiadriamycin and 2:1 4′-epiadriamycin-d-$(CGATCG)_2$ complex.

volve specific hydrogen bonding and van der Waal's interactions (Table 6). The root mean square deviation between the rMD structure and the starting structure is quite large but among various final structures is very low. This is an indication that convergence has been achieved. Table 7 indicates an assessment of refined structure in terms of energetics and distance deviation from the target distance. The total energy of the final structure is 146 kcal mol^{-1}, which is lower than the initial B-DNA structure. Table 8 shows the pair wise as well as residue wise root mean square deviations (RMSD) of the complex. The starting structure was chosen as reference and the value of target RMSD is chosen to be 0.0. It may be noted that distance deviation reached a minimum of 0.8 Å from an initial average deviation of 0.0 Å.

2.4.1. Conformation of DNA

All helical parameters, backbone torsional angles and sugar conformations of the resulting rMD structures were thoroughly analyzed with the program CURVES, version 5.1.[28,29] The plots of helicoidal parameters (global unless specified otherwise) are made as a function of residue position in the duplex, along with that for the classical structures of A-DNA and B-DNA and are shown in Figure 9a and b.

Among the base pair axis parameters, the *x*-displacement (d*x*) and *y*-displacement (d*y*) are found to vary to a large extent for all base pairs. The base pairs are inclined at an angle (η) up to 6°, the inclination being larger at 5′ end. The tip angle fluctuates along the base sequence. The variation in shear, stretch, stagger, and buckle is fairly large for the CG base pair at both the ends. The propeller twist at either ends are negative and large, indicating that the ends are not having fraying effects. The inter-base parameters shift (D*x*) and slide (D*y*), vary in the range −0.16 to +0.07 Å. The rise per residue (D*z*) is 3.25 Å at A3pT4 base pair step while that at C1pG2 and C5pG6 base pair step increases up to 6.3 Å to accommodate drug chromophore. The intercalation results in large amount of tilt (τ = 2.21° to −0.75°) in base pairs. The roll angle (ρ) varies from +10° to −3°. Positive roll opens the angle between the base pairs towards the minor groove; as a result a wider minor groove and bending towards major groove causing a curvature in the helix occurs. The large positive roll at C5pG6 (+10°), step indicates reduced base stacking at C5pG6 end. This is due to the fact that intercalating anthracycline ring chromophore is oriented approximately perpendicular to the base pair axis in the helix, as found in the crystal structures of the complexes. The A3pT4 base pair step shows negative value of the roll (−3°). The propeller twist is in the range from −6° to 29° out of which the terminals are having negative value as the drug is intercalating at the terminal ends. The local inter base parameters also show positive roll angle at both the ends of the helix and negative roll in the center. The twist (Ω) varies in the range 30.1–40.0°. The twist angle values at the intercalation steps indicate that there is unwinding of DNA at these

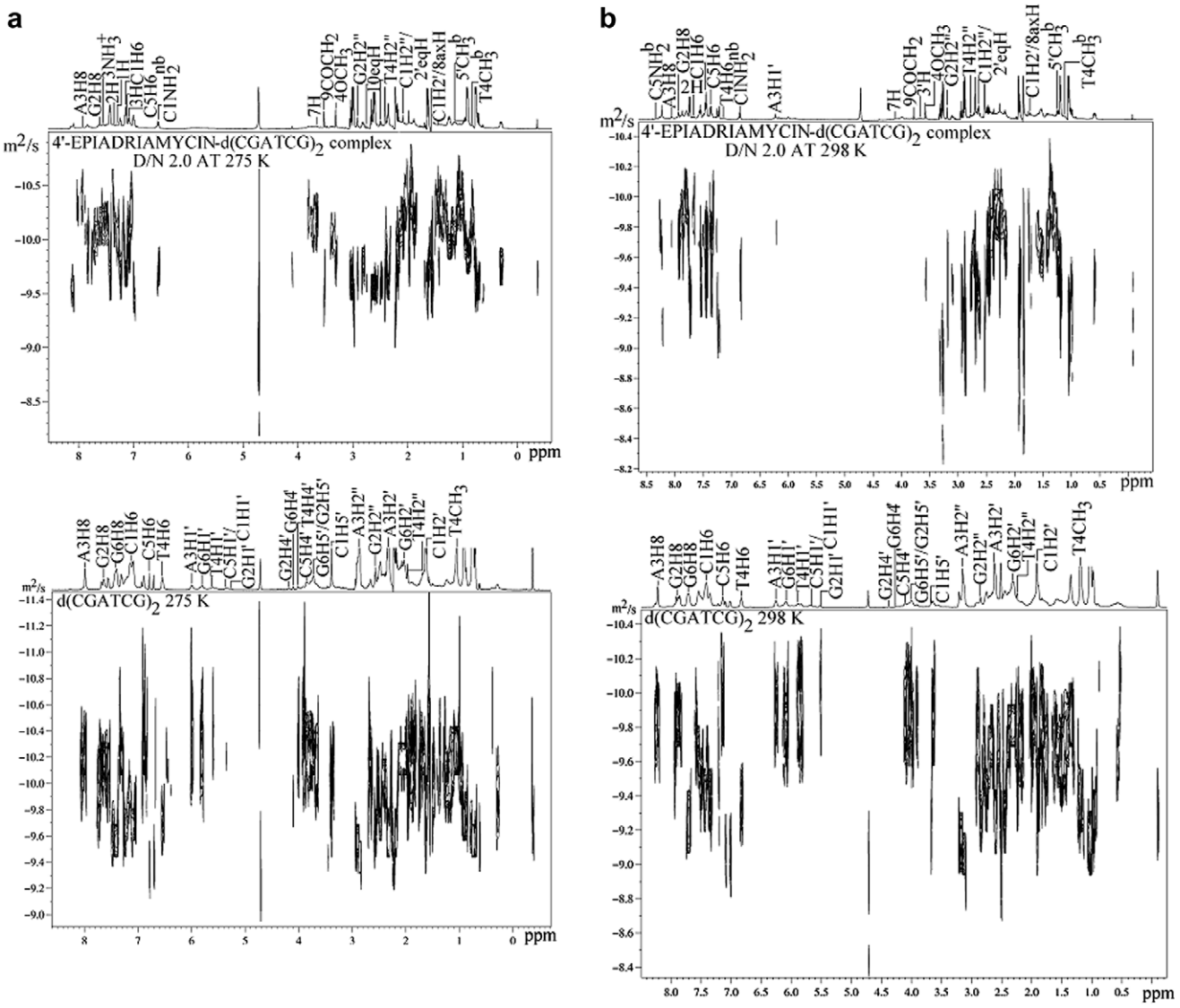

Figure 7. DOSY spectra of 4′-epiadriamycin-d(CGATCG)$_2$ complex and d(CGATCG)$_2$ at (a) 275 and (b) 298 K in D_2O.

steps. Also there is unwinding of DNA at the steps adjacent to the intercalation steps. The width and depth of major groove is found to be 12.48 and 4.53 Å while the corresponding values for minor groove are 6.05 and 5.00 Å, respectively. Thus, the minor groove is wider perhaps to allow proximity of daunosamine sugar moiety.

The backbone torsional angles along with the values for canonical B-DNA and A-DNA are plotted in Figure 10. The torsional angles α, β and γ adopt *gauche*$^-$, *trans* and *gauche*$^+$ conformations, respectively. The torsional angle ζ, however, deviates from the normal *gauche*-conformation and adopts a *trans* conformation for the G2 and C5 bases. This is due to the opening of base pairs at these sites. This is accompanied by a corresponding deviation in torsional angle ε for G2 and C5 bases to a lower negative value of 91° and 100°, respectively, as compared to a value to 155° found in B-DNA structures. The torsional angle, δ as well as pseudorotation phase angle *P*, is deviated from the normal range around C2′ *endo* conformation. The glycosidic bond rotation, χ, of the DNA molecule measuring rotation of base around sugar varies along base sequence. The χ angles are as follows: C1, 180°; G2, −108°; A3, −136°; T4, −118°; C5, −86°; G6, −82°. On C1pG2 side of the backbone, the 2′-deoxyguanidine residue on the 5′-end site changes the glycosyl angle from an anti (−98° in B-DNA) to a low anti value (−108°). At the same time by adjusting ε angle from a near *trans* (155° in B-DNA) to a lower value (−91°), it allows the adjacent bases to separate from 3.4 to 6.3 Å.

On the C1pG2 side, both nucleotide units maintain the glycosyl angle at *trans* (180°, −108°). But the ε value is changed from 155° to a near *gauche* (−91°) conformation in the G2 residue, it is possible to separate the neighboring G2 and C1 bases to a distance of ~6.3 Å. This can be achieved by coupling it with the rotation of the phosphodiester linkage from a normal *gauche*-, *gauche*-conformation to a *trans*, *gauche*-, as observed in X-ray crystallography[12,30–32] and NMR[16] structures of similar complexes. The change in phosphodiester linkage gets reflected in the backbone torsional angles ε, ζ, α and β. A correlation between these torsional angles has been found on the basis of a number of B-DNA crystal structures, which have shown that two conformational states are usually observed in B-DNA, namely BI and BII. The BI state is characterized by torsional angles α, −62°; β, 176°; γ, 48°; δ, 128°; ε, −176°; ζ −95°; and χ, −102° to −119°; while the BII state is characterized by α, −62°; β, 176°; γ, 48°; δ, 144°; ε, −114°; ζ, −174°; and χ, −89°. Our results show that both G2 and C5 residues tend to adopt BII conformation. The A3 and T4 residues remain in the more stable BI state. It has been reported earlier that the idealized

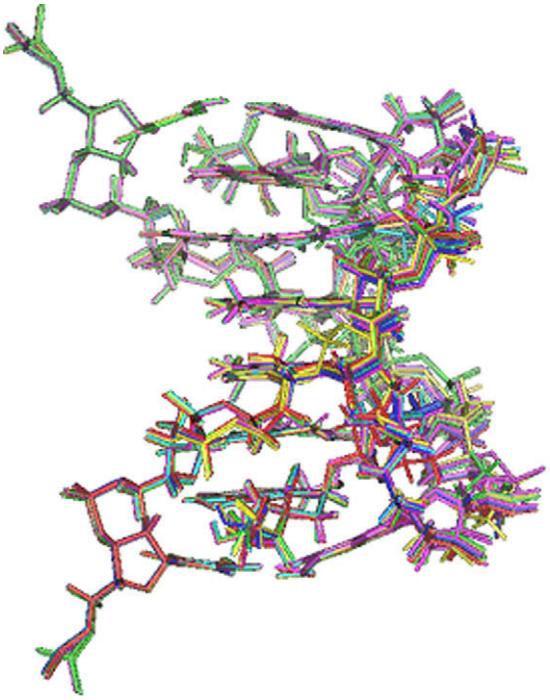

Figure 8. Superimposed structures of d-(CGATCG)$_2$-4′-epiadriamycin obtained by restrained molecular dynamics simulations.

Table 6
Close contacts (Å) between drug and DNA molecule

S. No.	Van der Waal's contacts		S. No.	H-Bond contacts	
	Protons	Distance		Protons	Distance
1	G2NH2^{b}–6O	2.07	1	C1N1–11O	2.94
2	G2C6–C10a	2.78	2	C1N3–12CO	2.82
3	G2C4–C11	2.72	3	G2N7–12CO	2.73
4	G2NH2^{nb}–O7	2.11	4	G2N7–11OH	2.41
5	G2N3–C10a	2.62	5	G2N9–11O	2.86
6	A3P–14OH	1.71	6	G2NH2^{b}–6O	2.07
7	T4P–4′OH	1.72	7	G2NH2^{nb}–O7	2.11
8	G6NH2^{b}–8axH	1.63	8	A3P–14OH	1.72
9	G6C6–C5	2.66	9	T4P–4′OH	1.73
10	G6C5–5CO	2.58	10	C5N3–5CO	2.54
11	G6C2–C6	2.76	11	C5O2–6OH	2.37
			12	G6N7–5CO	2.68
			13	G6N9–6O	2.88
			14	G6N3–6O	2.74

Table 7
Energy terms (kcal mol^{-1}) for starting model and final rMD structure

Energies (kcal mol^{-1})	d-(CGATCG)$_2$-4′-Epiadriamycin complex	
	Initial	Final
Total	1218	146
Bond	91	98
Angle	556	560
Dihedral	−46	−55
Van der Waal	138	179
Repulsion	2119	2179
Dispersive	−1981	−2000
Electrostatic	541	434
Restraint	203	189

g-g-conformation of phosphodiester bond from 5′ to 3′ direction changes *g-g-—tg-—g-g-—g-g-—tg-* (where *t* and *g-* stand for *trans* and *gauche-*, respectively) in X-ray crystallographic[13] and NMR structures[16] in hexamer sequences d-CGATCG and d-CGTACG on binding to similar drugs. The trans, *gauche*-conformation in G2pT3 or G2pA3 step in X-ray structure[12,13] is associated with change in β angle of T4/A3 residue (adjacent to intercalating bases) to 120–138°. Further in these complexes, pseudorotation P = 105° for T4 residue or δ angle of 72–92° for A3 and T4 residues have been reported. The corresponding δ or P for T4 residue in our case is 117–126°. Thus intercalation of 4′-epiadriamycin induces and stabilizes a distinct pattern of phosphates of the DNA backbone. There appears to be a possibility to directly influence the DNA backbone through complexation, hence leads to a redirection of intercalation caused structural changes to the backbone, as proposed in literature.[17]

2.4.2. Conformation of 4′-epiadriamycin

The bond distance and angles in the 4′-epiadriamycin molecule are within the limits of accepted values. In the aglycon part of the molecule, the B and D rings are most aromatic with an averaged C–C distance of 1.40 Å. The distance between O5 and O6 atoms and between O11 and O12 atoms are 1.75 and 1.88 Å, respectively; they presumably form intramolecular hydrogen bonds. The aromatic part of the aglycon is quite planar with rms distance of 0.80 Å for the least squares plane calculated from all the atoms of rings B, C, and D without the exocyclic atom. The methyl group in the 4-methoxy side chain is also in plane with a deviation of 0.78 Å. The orientation of methoxy group is such that the methyl group is pointed away from O5 atoms and protrudes into the solvent region. The torsional angles of the 4′-epiadriamycin molecule in the complex (Table 9) are different from that of daunomycin in the free state[33] and in the same/similar bound complexes.[12,31] In ring A, the torsional angles around C19–C20 (5–8°) and C20–C7 (28–35°) bonds are negligible while that around C8–C9 (45–50°) and C9–C10 bonds are (−13° to −16°) in magnitude. Thus, practically all atoms except C9 atom are out of the plane containing other atoms and aromatic rings B, C, and D. The C9 atom is displaced by 0.89 Å in same direction as the amino sugar relative to the plane of aglycon molecule as a consequence of which 9OH can no longer form intramolecular hydrogen bond with 7H atom. The torsional angles corresponding to *O*-glycosyl linkage, C20–C7–O7–C1′ and C7–O7–C1′–C2′, are lower (−137°, 168°) than the corresponding angles in the pyridine salt of daunomycin molecule[34] in the free state (−114°, 167°). The amino sugar is in a chair conformation with all the side chains pointing away from the aglycon. The torsional angle around C1′–C2′ bond (39°) is shorter than the expected *gauche* value in the six-membered rings.

2.5. Comparative analysis of 4′-epiadriamycin-d-(CGATCG)$_2$ and other anthracycline–DNA complexes

A view showing the stacking interactions is shown in Figure 11. There are significant deviations from twofold symmetry relating the backbone of the B-DNA molecules. The G2.C11 base pair is translated towards minor groove by ~1.3 Å and tilted with respect to A3.T10 base pair. The A3.T10 base pair is translated along long axis of the base pair by about 1 Å with respect to next base pair along 5′–3′ direction.

The drug is positioned with respect to DNA molecule (Fig. 12a and b) such that the hydroxyl oxygen atom of 9OH in ring A is within the hydrogen bonding distance of N3 and N2 atoms of guanine base G2. However, there is existence of weak hydrogen bonding. The distance between O9 and G2N3 atom is 3.93 Å and varies in the range 3.5–4.7 Å in 100 structures saved at equal intervals during 100 ps rMD simulations. The distance of O9 from G2N2 atom is 4.01 Å and varies in the range 4.0–4.5 Å so that this hydrogen bond is rather weak. O7 atom of 4′-epiadriamycin which links the chromophore and amino sugar, is close to N2 of G2 residue with the separation of 3.0 Å while O9 is far from O4′ of G2

Table 8
Summary of experimental restraints and statistical analysis of final structure generated by restrained molecular dynamics (rMD)

Parameters	No. of distance restraints
Intra residue	172
Inter residue	62
Total NOE violations	31
Average pairwise RMSD	Initial = 0.0; final = 0.76
Average residue wise RMSD	C1 = 0.058, G2 = 0.078, A3 = 0.047, T4 = 0.053, C5 = 0.055, G6 = 0.083
Minor groove	Width = 7.22 Å; depth = 4.85 Å
Major groove	Width = 13.09 Å; depth = 1.95 Å

(4.2 Å). The distance of O7 atom from O9 atom of 9OH hydroxyl group in ring A is 2.87 Å so that there is possibility of intramolecular hydrogen bond between O7 and 9OH. Apparently in order to have hydrogen bond of O9 with G2N3, the ring conformation is altered in a specific way, which moves O7 atom away.[30] This hydrogen bonding interaction is likely to be sensitive to conformation of ring A. The distance between O9 atom of 9CO and O2 of C1 in our structure is 5.11 Å so that bridging of O9 atom of 9CO to O2 of C1 through water may not be possible. Further the distance between O4 and O–1P of G6 is 8.97 Å. However the distance between O5 and C5N1 is 3.24 Å. A hydrogen bond involving O4 and O5 atoms with phosphate groups of G6 are possible through two water molecules acting as bridges between them. In our rMD structures these N–H···O distances from C5O2, C5O4′, and T4O2 atoms are 3.61, 3.98, and 4.76 Å, respectively. We have therefore looked into these contacts throughout the course of simulations. It is found that the distance of NH_3^+ from C5O2, C5O4′, and T4O2 are in the range 3.5–4.3, 3.8–4.3, and 3.9–5.0 Å, respectively. At the other intercalation site, the distance of NH_3^+ from C11O2, C11O4′, and T10O2 are in the range 4.2–4.9, 4.5–5.1 and 4.6–5.1 Å, respectively. If we consider 3.5 Å as the cut off distance for hydrogen bond then NH_3^+ moiety is able to make at the most two hydrogen bonds. The distance of NH_3^+ from O4′ of T4/T10 and N3 of A3/A9 are in the range 5.0–6.5 and 4.5–5.0 Å, respectively, so that there are no contacts through hydrogen bonds between these groups of atoms, as seen in some X-ray crystal structures.[13,30,31]

An interesting feature of daunomycin/adriamycin/4′-epiadriamycin is its flexibility of O-glycosidic bond rotation C7–O7–C1′–C2′. Throughout the course of simulations, we find that the O-glycosidic angle C7–O7–C1′–C2′ remains within a narrow range of angles, 165–180°, and stabilizes at 168°. In uncomplexed daunomycin and its analogues it is found to be 162–168[33,35–37] while in the X-ray crystal structure of adriamycin complexed with d-CGATCG it is 148° and in some complexes, for example, 4′-epiadriamycin complexed with d-TGATCA and daunomycin with d-CGATCG it is 132–137°.[14,38] In most other crystal structures, it is 145–161°.[15,31,32] The molecular dynamics simulations have however shown[17] that a much lower dihedral angle, 57–61°, is also accessible. In the first conformation centered at 159°, the nitrogen of the ammonium group is at a distance of 5.5, 5.1, and 3.2 Å from C5O4′, T4O2, and T4O4′, respectively, while in the second centered at 137°, the corresponding distances are 3.2, 3.0, and >6 Å, respectively. In the third conformation centered at 59°, the distance of nitrogen of NH_3^+ from G6O4′ and G6O5′ are 3.4 and 3.0 Å, respectively. The energy barrier between 137° and 159° conformations is 0.3–0.7 kcal mol^{-1} and that between 137° and 59° conformations is 1.4 kcal mol^{-1}. Apparently in our case, the first and second substrates were kinetically readily accessible. The observed distance of nitrogen of NH_3^+ from C5O4′/C11O4′, T4O2/T10O2, and T4O4′/T10O4′ is in the range 3.1–5.1 Å and that from G2O4′ and G2O5′ is in the range of 9–12 Å.

During the course of simulations, it is observed that hydrogen atom of 6OH group of ring B of 4′-epiadriamycin points towards O5 atom (that is away from O7 atom) in 98 out of 100 structures while hydrogen of 11OH points towards O12 and is away from C10 position. Apparently 6OH···5O hydrogen bond is only stabilized in the drug–DNA complex. This is similar to the existence of both hydrogen bonds in the uncomplexed daunomycin, adriamycin, and 4′-epiadriamycin investigated by us. The position of H atom of 6OH remains fixed and is not correlated to O-glycosidic bond rotation C7–O7–C1′–C2′ which while varying in the range 165–180°, positions the daunosamine sugar moiety close to 6OH in different orientations. The stabilization of 6OH···5O hydrogen bond thus ensures a fixed position of hydrogen atom of 6OH which has been found to be close to C5H1′ (distance 3.24 Å) of DNA. Besides this, several other contacts O5–C5H1′, O6–C5H1′, O5–C5H2′, $4OCH_3$–C5H2′, 6OH–C5H1′, having distances within 4.0–5.0 Å, establish the involvement of $4OCH_3$, O5, O6, and 6OH atoms in stabilizing the drug–DNA complex. Some of the contacts, also observed earlier,[30] for example, 10axH with C1O2; 10eqH with G2N3; 3′H with G2N2; 2′axH with C5O2, have an important role in binding.

4′-Epiadriamycin drug differs from daunomycin by a hydroxyl group attached at C14 position, that is, presence of $9COCH_2OH$ group as compared to $9COCH_3$ group in daunomycin and inversion of 4′OH at the daunosamine sugar moiety. In the rMD structure of the complex, it is observed that the hydroxyl group makes short van der Waal's contact with A3H5′ (3.01 Å) and A3H4′ (4.89 Å). Its distance from G2O3′ and G2 phosphorus atom is 4.66 and 3.98 Å (Table 6), respectively. This group has been implicated in binding to phosphate through water bridge in X-ray crystal structure of adriamycin with d-CGATCG.[12] Thus we find that 5O, $4OCH_3$, 6OH and O7 groups are involved in drug–DNA interactions (Fig. 13). This may require existence of 6OH···5O and 11OH···12O hydrogen bond. Involvement of NH_3^+ group in interaction is related to conformation of O-glycosidic bond. The binding to DNA through 9CO, 9OH, and $9CH_2OH$ groups depends upon ring A conformation. Presence of 11OH···12O hydrogen bond may not be critical for binding and atoms of position 1, 2, 3, 12, and 11 are not involved in drug–DNA interactions.

2.6. Biological and medicinal relevance

The anthracycline antibiotics are among the most effectual antitumor medicines used for medicinal treatment of various types of malignant tumors. It is well known that 4′-epiadriamycin is better tolerated, active against a variety of solid tumors with reduced cytotoxicity and lesser side effects. This drug is localized in the nucleus and shows cytotoxic and anti-mitotic activity. Orientation of the functional groups attached at C9 position on aglycone ring A and daunosamine sugar moiety was found to be different on the formation of the complex. The 4′-OH of daunosamine sugar forms additional hydrogen bonds as compared to that in daunomycin[13,30,31] and adriamycin[12] complexes. The role of drug–DNA covalent bonding in cells was also investigated with synthetic epidoxorubicin–formaldehyde (Epidoxoform) and synthetic daunorubicin–formaldehyde (daunoform) conjugate. It was observed that the fluorophore of daunoform appeared more rapidly in cells and was released more rapidly from cells than the fluorophore of epidoxoform. Epidoxoform was found to be threefold more toxic to MCF-7 human breast cancer cells and greater than 120-fold more toxic to MCF-7/adriamycin resistant cells than that for epidoxorubicin.[39,40]

The cardiotoxicity of these anthracycline drugs are known to be due to the ability to generate oxygen radicals during redox cycling and in vitro reductive glycosidic cleavage through the formation of tautomer 7-deoxydaunomycinone.[41,42] The kinetics of sugar moi-

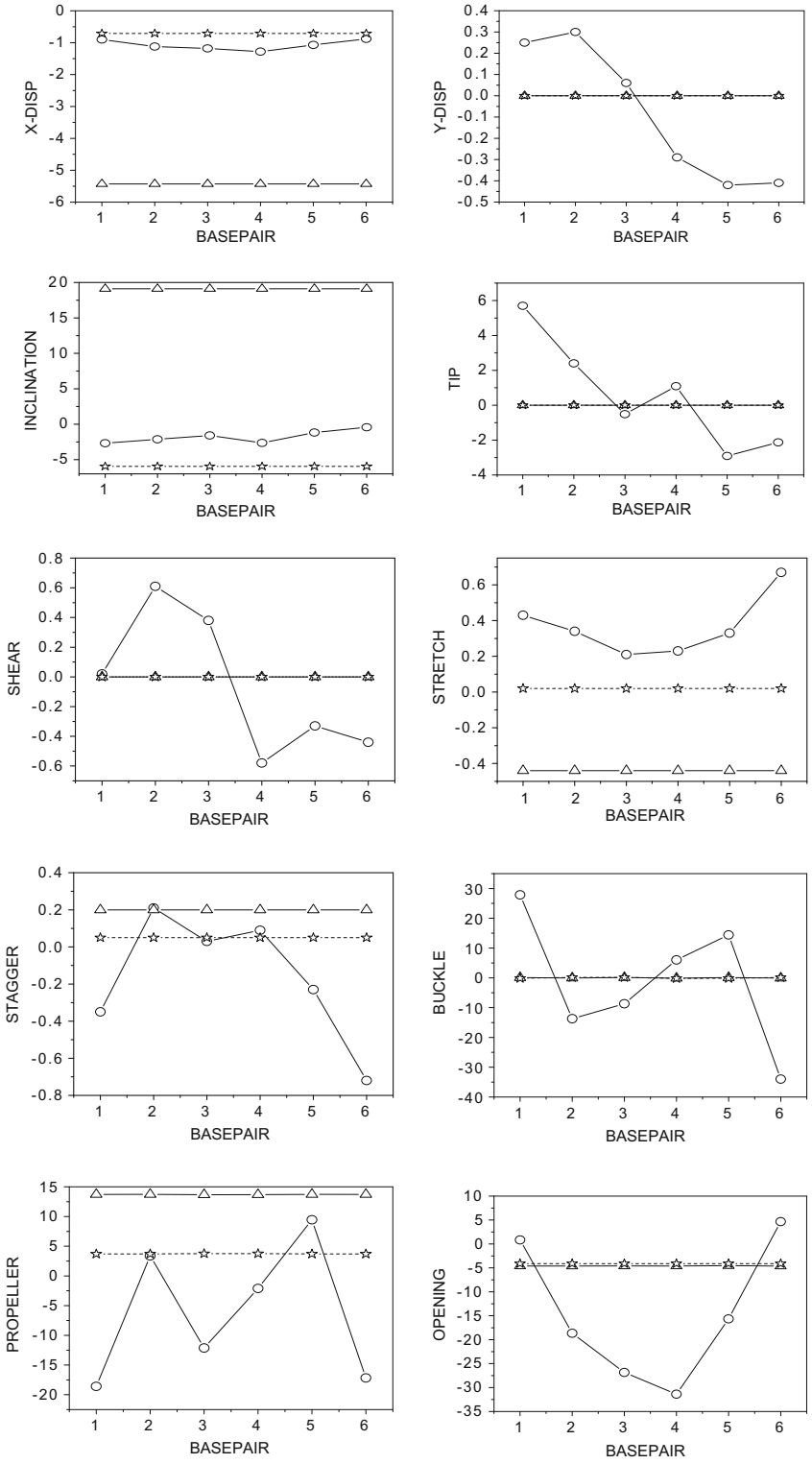

Figure 9. (a) and (b) Helical parameters for d-(CGATCG)$_2$ complexed with 4′-epiadriamycin calculated for structure obtained by restrained molecular dynamics simulations (–○–) and that for standard A-DNA (–△–), B-DNA (–☆–).

ety detachment has been related to conformation of cyclohexyl ring A.[43] The mass spectrometric studies[44] on the anthracycline drugs have given a direct proof of negligible glycosidic cleavage in 4′-epiadriamycin. These results may well explain why 4′-epiadriamycin developed recently is better tolerated due to lesser cardiotoxicity than adriamycin and daunomycin.

3. Summary and conclusions

Large upfield shifts are observed in C1H1′, G2H1′, G2NH, G6NH and G6H2′ protons on binding of drug to DNA hexamer sequence. The 1H, 2H, 3H, 7H protons of the drug are shifted downfield up to 0.6 ppm while the sugar protons 3′H, 4′H and 6OH are shifted

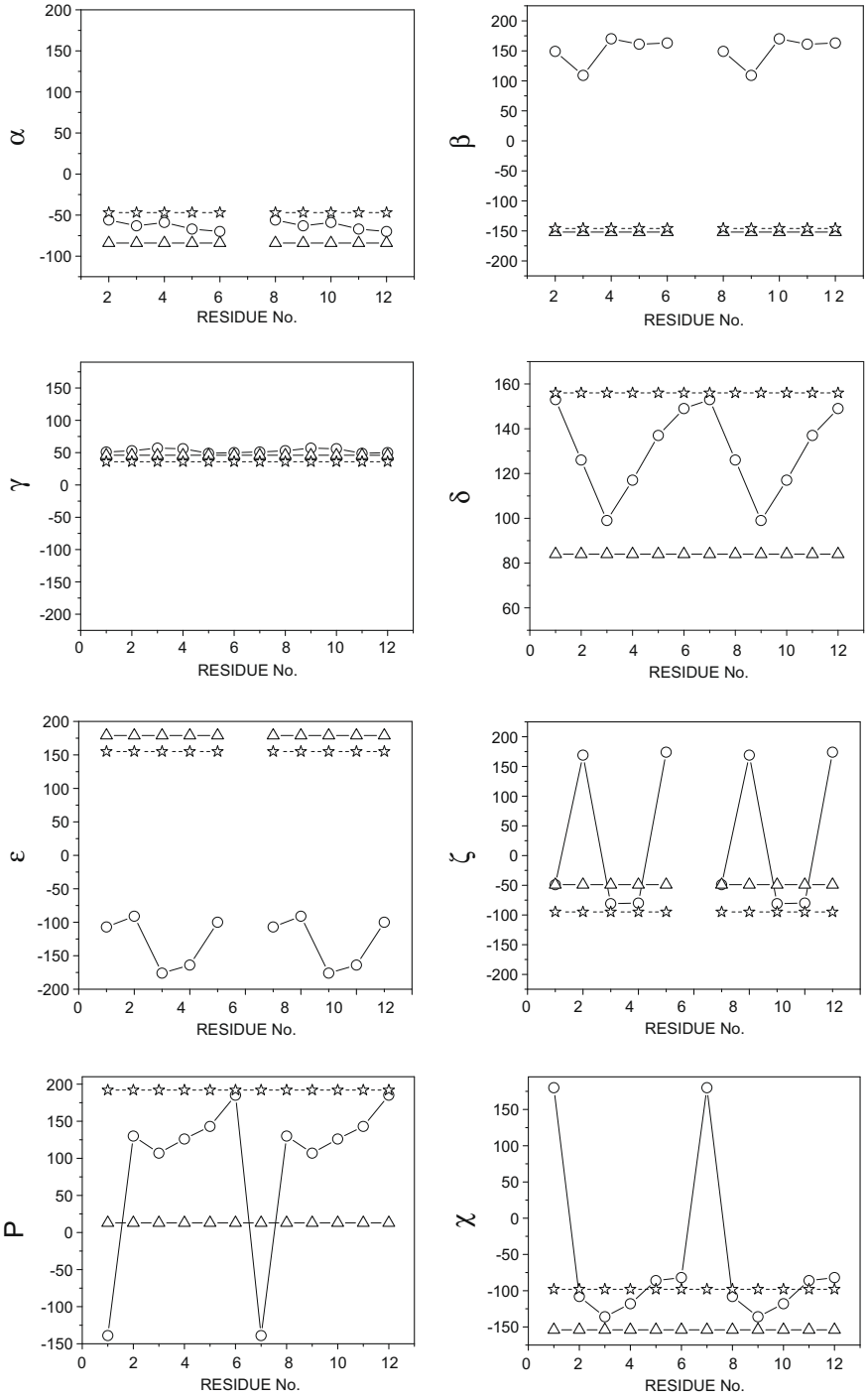

Figure 10. Backbone torsional angles for d-$(CGATCG)_2$ complexed with 4′-epiadriamycin calculated for structure obtained by restrained molecular dynamics simulations (–○–) and that for standard A-DNA (–△–), B-DNA (–☆–).

downfield up to 0.9 ppm in the complex. Sequential NOE (nuclear Overhauser effect) connectivities between C1pG2 and C5pG6 steps are not observed as the drug chromophore intercalates at these base pair steps. Presence of several other intermolecular NOEs corroborates the same. BI–BII transition has been detected at these base pair steps. The observed sequence dependant variations in DNA occur presumably to allow intercalation of the drug chromophore. The conformation of the drug also changes in order to have interaction with G2 base. Our studies establish the role of 9OH, 9CO, NH_3^+, 7O, $4OCH_3$ groups in binding to DNA. The observed NOEs and short interproton distances in the solution structure of the complex confirm that the anthraquinone ring intercalates between CG base pairs excluding 3 base pairs adjacent to it. Besides this, lifetime measurement study has been done to show that there is shortening of decay time on complex formation. The DOSY spectral analysis also shows that the rate of diffusion decreases due to the binding of drug to DNA hexamer. The present study is the first rMD study on the solution structure of 4′-epiadriamycin with d-$(CGATCG)_2$ hexamer. The rMD simulations of 4′-epiadriamycin-d-$(CGATCG)_2$ complex based on intermolecular and intramolecular NOEs have led to a detailed conformational analysis. The intercalation of drug chromophore at d-CpG steps is stabilized by stacking

Table 9
Selected torsional angles (°) of the 4′-epiadriamycin in the complex and their comparison with similar structures available in literature

Torsional angles	Present work CGA + 4′-*epi*	TGA + dnm[a]	TGT + dnm[b]	TGA + 4′-*epi*[c]	TGT + 4′-*epi*[d]	dnm[e]
Ring A						
C6a–C7–C8–C9	−58	−56	−40	−45	−50	−48
C7–C8–C9–C10	50	66	55	68	63	58
C8–C9–C10–C10a	−15	−35	−44	−60	−42	−38
C9–C10–C10a–C6a	−14	−2	27	33	14	14
C10–C10a–C6a–C7	5	10	−11	−8	−1	−5
C10a–C6a–C7–C8	30	18	14	13	18	20
Glycosyl						
C8–C7–O7–C1′	96	129	120	96	95	125
C6a–C7–O7–C1′	−137	−115	−125	−139	−142	−114
C7–O7–C1′–O5′	−64	−115	−105	−102	−81	−68
C7–O7–C1′–C2′	168	127	137	132	159	167
Amino sugar						
O5′–C1′–C2′–C3′	39	−49	−60	−31	−53	−54
C1′–C2′–C3′–C4′	−57	50	49	41	52	56
C2′–C3′–C4′–C5′	16	−20	−17	−53	54	−61
C3′–C4′–C5′–O5′	44	−16	−5	61	57	61
C4′–C5′–O5′–C1′	−67	19	−9	−55	−59	−59
C5′––O5′–C1′–C2′	24	17	42	36	57	57

[a] TGATCA + daunomycin.[13]
[b] TGTACA + daunomycin.[13]
[c] TGATCA + 4′-epiadriamycin.[14]
[d] TGTACA + 4′-epiadriamycin.[15]
[e] Daunomycin.[33]

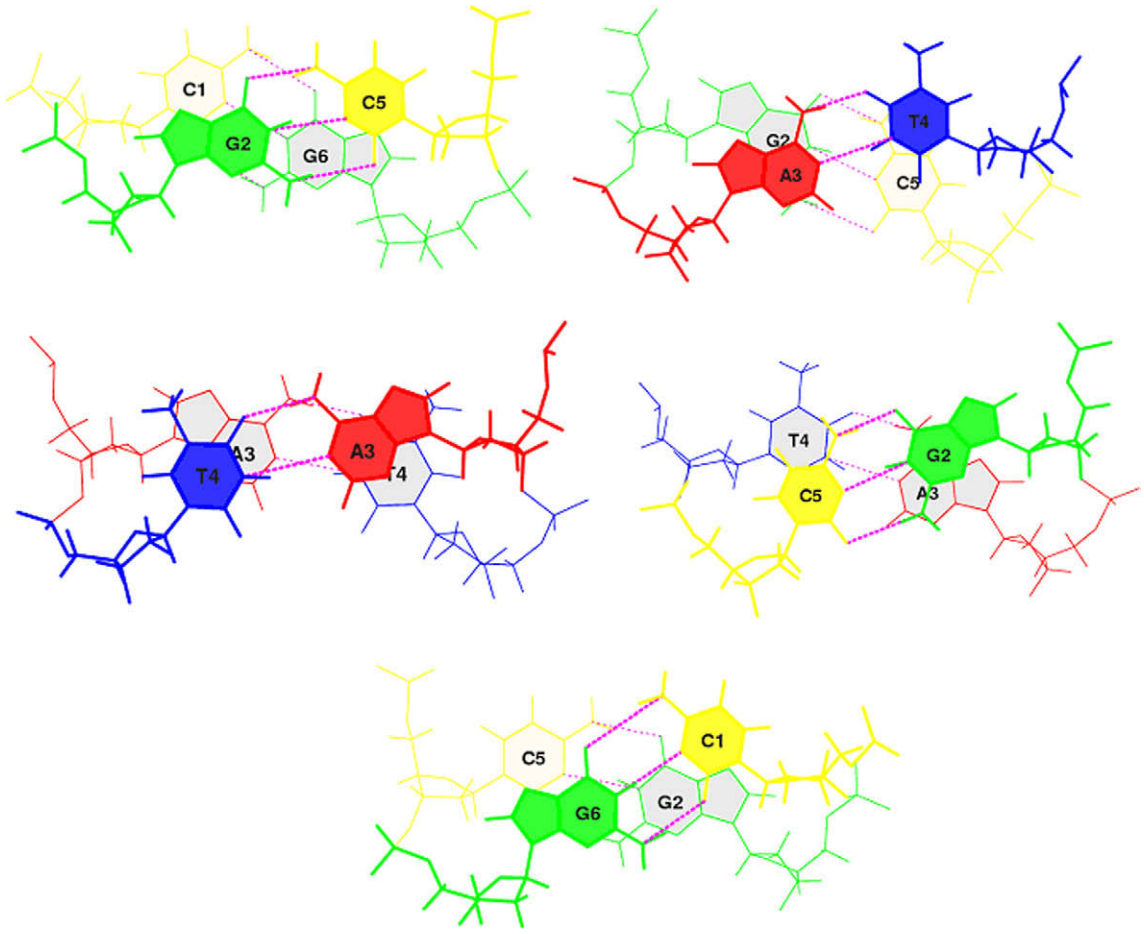

Figure 11. Overlap of base pairs at different base pair steps in d-$(CGATCG)_2$-4′-epiadriamycin complex showing stacking interactions.

interactions while several other hydrogen bonds and van der Waal's interactions involving O5, 6OH, and NH_3^+ moiety of daunosamine sugar, and rings A protons stabilize the drug–DNA complex. The O9 atom is involved in hydrogen bond formation with G2N3 and G2N2H while O7 atom has close contact with G2N2 atom. The O-glycosidic bond C6a–C7–O7–C1′ is stabilized around

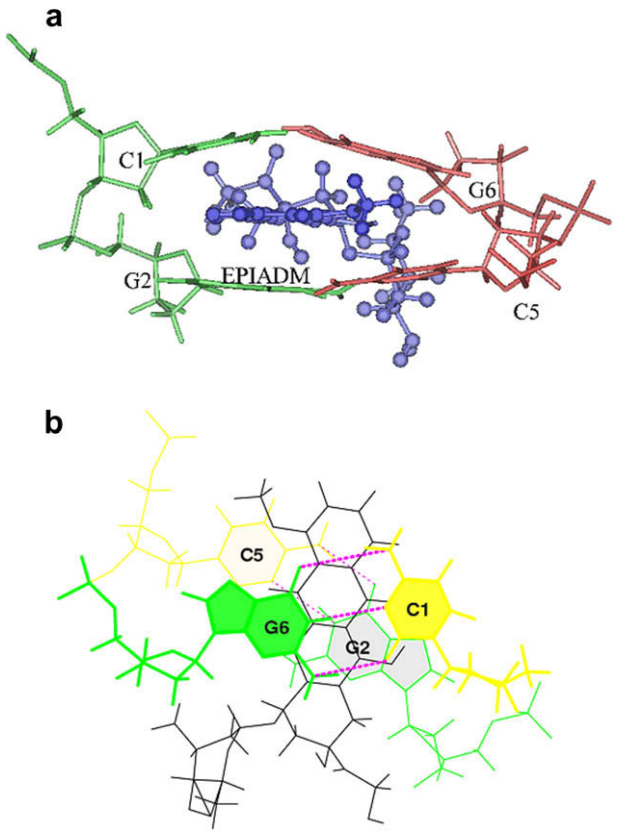

Figure 12. Drug–DNA stacking interaction in the intercalation site showing the orientation of the 4′-epiadriamycin with respect to base pairs (a) front view (b) top view.

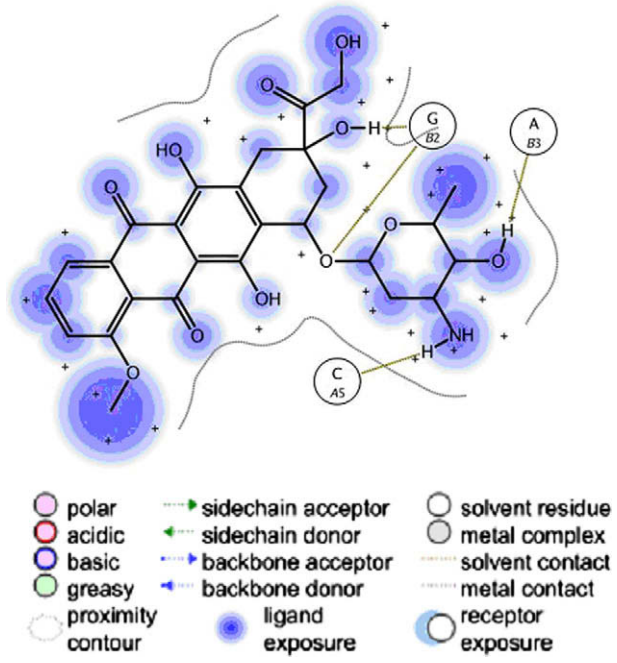

Figure 13. Various interactions present in 2:1 4′-epiadriamycin-d-$(CGATCG)_2$ complex.

137°. The conformation of O-glycosidic bond and ring A is related to cleavage of C7–O7 bond and subsequent production of free radicals which are responsible for cardiotoxicity. Therefore, any substitution in ring A or daunosamine sugar will affect the binding (and hence anti cancer action) as well as cell toxicity. These findings can provide leads for designing drugs of higher potency, reduced cell toxicity, and decreased resistance to tumor cell lines and hence find potential medical applications.

4. Experimental

The deoxyribonucleic sequence d-$(CGATCG)_2$ was purchased from Microsynth, Switzerland. Deuterium oxide (D_2O), with isotopic purity 99.96% and 4′-epiadriamycin were purchased from Calbiochem Pvt. Ltd, San Diego, USA. Sodium 2,2-dimethyl-2-silapentane-5-sulfonate (DSS), an internal NMR reference was purchased from Merck Sharp and Dohme Canada Ltd, Canada. All other chemicals like Na_2HPO_4 and NaH_2PO_4 and ethylene diamine tetra acetic acid (EDTA) are of analytical grade and purchased from E. Merck, India Ltd. Solution of 4′-epiadriamycin (88.33 mM) was prepared by dissolving a known quantity of sample in 90% water and 10% D_2O. The final concentration is checked by absorbance measurements at wavelength of 480 nm using Cary Bio 100 Spectrophotometer. The extinction coefficient (ε value used for 4′-epiadriamycin is $\varepsilon = 11{,}500\ M^{-1}\ cm^{-1}$. Solution of deoxyoligonucleotide, d-$(CGATCG)_2$ (4.62 mM, duplex concentration) was prepared by dissolving a known quantity of sample in deuterated phosphate buffer (20.0 mM) of pH 7.0 having 50 mM Na salt. The sample of d-$(CGATCG)_2$ was dissolved in 540 μl of deuterated phosphate buffer and 60 μl of D_2O and its concentration was determined by absorbance measurements at 260 nm. Using extinction coefficient (ε value = $57{,}200\ M^{-1}\ cm^{-1}$. Ethylene diamine tetra acetic acid (EDTA), 0.1 mM, was added to suppress any paramagnetic impurity, which may cause line broadening during NMR measurements. Typically 1 μl of 0.1 M solution of DSS was added to the complex of d-$(CGATCG)_2$ and 4′-epiadriamycin as an internal reference. 4.62 mM d-$(CGATCG)_2$ and 88.33 mM 4′-epiadriamycin samples were taken as a stock solution for preparation of complex. A complex of d-$(CGATCG)_2$ and 4′-epiadriamycin was prepared by titration. 65 μl of 88.33 mM 4′-Epiadriamycin was added in steps of 5 μl to 0.6 ml of 4.62 mM d-$(CGATCG)_2$ sample during titration in order to make the complex of 4′-epiadriamycin: d-$(CGATCG)_2$ D/N = 0.16, 0.32, 0.48, 0.64, 0.80, 0.96, 1.11, 1.27, 1.43, 1.53, 1.60, 1.75, 1.91 and 2.03. All proton NMR experiments were carried out at Central NMR Facility, Indian Institute of Technology Roorkee and recorded on 500 MHz high resolution Bruker Avance 500 FT-NMR spectrometer equipped with computer having Topspin (1.3 version) software. Typical parameters for one-dimensional NMR experiments are: pulse width = 10–12.5 μs (30° pulse); no. of data points = 128–256 K; spectral width = 5000 Hz; no. of scans = 64–128 and digital resolution = 0.25–0.5 Hz/point. Receiver gain was optimized in each instance to obtain the best signal to noise ratio. In temperature variable experiments, constant temperature is maintained in the range 275–328 K using temperature control accessory. 2D phase-sensitive DQF COSY and NOESY experiments on d-$(CGATCG)_2$ and its complex with 4′-epiadriamycin were carried out at 275 K in 90% H_2O and 10% D_2O. 2D NOESY experiments were recorded with variable mixing times (τ_m) 100, 200 and 300 ms for 4′-epiadriamycin–d-$(CGATCG)_2$ complex. Typical parameters for 2D experiments were: 2 K data points along t_2 dimension; 512 free induction decays in t_1 dimension; pulse width ≈ 9.5–12 μs; spectral width ≈ 5000 Hz; no. of scans = 64–128; digital resolution 2.30–4.60 Hz/point and relaxation delay ≈ 2.0 s. Cross peaks in the NOESY spectra were integrated and intensities were translated into inter-proton distances using H5–H6 cross peak of cytosine as the reference distance = 2.46 Å; a range of ±0.5 Å was provided to account for any error in integration. Pseudo atom corrections were used for methyl and other

equivalent protons. The NOEs were categorized as very strong (ss), strong (s), medium (ws) and weakly (w) intense with the corresponding distances set in the range of ss 1.8–2.5 Å, s 2.5–3.0 Å, ws 3.0–3.5 Å, w 3.5–4.0 Å, ww 4.0–5.0 Å for the respective protons.

Time-resolved fluorescence measurements: Time resolved fluorescence decays were obtained by the time-correlated single-photon counting method on the Spectrofluorometer (model FluoroLog-TCSPC, make HORIBA Jobin Yvon Spex), used for the life time measurement study. The excitation source (λ_{ex} = 470 nm) was a fixed-wavelength Nano LED. The emission was detected at the emission wavelength (λ_{em} = 593 nm). The fluorescence emission of 4′-epiadriamycin and its complex with d-$(CGATCG)_2$ was counted by a micro channel plate photo multiplier tube, after passing through the monochromator and processed through constant fraction discriminator (CFD), time-to-amplitude converter (TAC) and multi channel analyzer (MCA). All measurements were performed at 298 K in water. The fluorescence decay was obtained and further analyzed by using the software, DAS, provided by FluoroLog-TCSPC instrument.

Diffusion ordered spectroscopy (DOSY): The DOSY experiment is the measure of diffusion coefficients by NMR. The relation between translational self-diffusion and the measurable NMR parameters[19] is:

$$A/A_0 = \exp[D_t\gamma_H^2\delta^2G_z^2(\Delta\delta/3)]$$

where A is the measured peak intensity (or volume), A_0 is the maximum peak intensity, D_t is the translational diffusion constant (in cm^2/s), γ_H is the gyromagnetic ratio of a proton ($2.675197 \times 10^4\ G^{-1}\ s^{-1}$), δ is the duration of the gradient, Δ is the time between gradients and G_z is the strength of the gradient (in G/cm). Data can be plotted as $-\ln(A/A_0)$ versus $\gamma_H^2\delta^2G_z^2$ $(\Delta - \delta/3)$. The slope of the line gives the value of D_t. The pulse program used is pulsed gradient spin echo (stimulated echo sequence incorporating bipolar gradients) sequence modified with binomial water suppression. The gradient strengths were incremented as a square dependence in the range from 1 to 32 G cm^{-1}. The diffusion time (Δ) and the duration of the magnetic field gradients (δ) were 100 ms and 6 ms, respectively. Other parameters include a sweep width of 6000 Hz, 32 K data points, 1024 transients and an acquisition time of 2.7 s and relaxation delay of 2.0 s. It has been developed in order to facilitate the complex mixture analysis without physical separation. This experiment will monitor molecular events such as molecular interactions or associations.

Restrained molecular dynamics methodology: The initial structure of d-$(CGATCG)_2$ was built using the biopolymer module in INSIGHT II, version 2005 (Accelrys Inc., San Diego, California) on Silicon Graphics Fuel workstation. The force constant was fixed as 40 kcal mol^{-1} $Å^{-2}$ for hydrogen bonds during the simulation. The energy of the molecule was minimized using 1000 steps each of Steepest Descent and Conjugate Gradient to remove any internal strain due to short contacts in starting structure using CFF91 force field in DISCOVER software version 2005 (Accelrys Inc., San Diego, California). Dielectric constant was fixed as 1.0 for calculation of electrostatic interactions. Conformational search was performed using the following simulated annealing restrained molecular dynamics protocol. The molecule was heated to a temperature of 800 K in steps of 100 K so that the chances of molecule being trapped in local minima become least and it can reach global minima. Molecular dynamics was carried out for 100 ps (1000 iterations with time step of 1 fs) at 800 K during which 100 structures were saved at regular intervals of 1 ps. Each of them was then slowly cooled at 300 K in steps of 100 K. The force constants for NOEs for strong, medium and weak peaks were held constant as 25, 15 and 10 kcal mol^{-1} $Å^{-2}$, respectively. At the end of simulated annealing all the structures were minimized by 1000 steps of Steepest Descent until a predefined convergence limit of root mean square derivative of <0.001 kcal mol^{-1} $Å^{-1}$ was reached.

Acknowledgments

The use of 500 MHz FT NMR Facility at Indian Institute of Technology Roorkee, Roorkee is gratefully acknowledged. The authors gratefully acknowledge Council of Scientific and Industrial Research (CSIR), Govt. of India, for a Senior Research Fellowship to Prashansa Agrawal.

Supplementary data

Supplementary data associated with this article can be found, in the online version, at doi:10.1016/j.bmc.2009.02.032.

References and notes

1. Arcamone, F. In *Anticancer Antibiotics, Medicinal Chemistry*; Crooke, S. T., Reicin, S. D., Eds.; Academic Press: New York, 1981; p 1.
2. Neidle, S. *Prog. Med. Chem.* **1979**, *16*, 151.
3. Di Marco, A.; Arcamone, F.; Zunino, F. In *Antibiotics*; Corcoran, J. W., Hahn, F. E., Eds.; Academic Press: New York, 1974; p 101.
4. Penco, S.; Arcamone, F. *Molecular Aspects of Anticancer Drug Action*; Macmillan Press: London, 1988.
5. Patel, D. J. *Biopolymers* **1979**, *18*, 553.
6. Phillips, D. R.; Roberts, G. C. K. *Biochemistry* **1980**, *19*, 4795.
7. Davies, D. B.; Eaton, R. J.; Baranovsky, S. F.; Veselkov, A. N. *J. Biomol. Struct. Dyn.* **2000**, *17*, 887.
8. Chaires, J. B. *Biopolymers* **1985**, *24*, 403; Chaires, J. B.; Dattagupta, N.; Crothers, D. M. *Biochemistry* **1982**, *21*, 3933; Pachter, J. A.; Huang, C. H.; Du Vernay, V. H.; Prestayko, A. W.; Crooke, S. T. *Biochemistry* **1982**, *21*, 1541.
9. Xodo, L. E.; Manzini, G.; Ruggiero, J. *Biopolymers* **1988**, *27*, 1839; Dalgleish, D. G.; Fey, G.; Kersten, W. *Biopolymers* **1974**, *13*, 1757.
10. Chen, K. X.; Gresh, N.; Pullman, B. *Nucleic Acids Res.* **1986**, *14*, 2251.
11. Chaires, J. B.; Herrera, J. E.; Waring, M. J. *Biochemistry* **1990**, *29*, 6145.
12. Frederick, C. A.; Williams, L. D.; Ughetto, G.; van der Marel, G. A.; van Boom, J. H.; Rich, A.; Wang, A. H. J. *Biochemistry* **1990**, *29*, 2538.
13. Nunn, C. M.; Meervelt, L. W.; Zhang, S.; Moore, M. H.; Kennard, O. *J. Mol. Biol.* **1991**, *222*, 167.
14. d'Estaintot, L.; Bernard, G.; Brown, T.; Hunter, W. H. *Nucleic Acids Res.* **1992**, *20l*, 3561.
15. Leonard, G. A.; Brown, T.; Hunter, W. N. *Eur. J. Biochem.* **1992**, *204*, 69.
16. Mazzini, S.; Mondelli, R.; Ragg, E. *J. Chem. Soc., Perkin Trans. 2* **1998**, 1983.
17. Trieb, M.; Rauch, C.; Wellenzohn, B.; Wibowo, F.; Loerting, T.; Mayer, E.; Liedl, K. R. *J. Biomol. Struct. Dyn.* **2004**, *21*, 713.
18. Barthwal, R.; Agrawal, P.; Tripathi, A. N.; Sharma, U.; Jagannathan, N. R.; Govil, G. *Arch. Biochem. Biophys.* **2008**, *474*, 48.
19. Stejskal, E. O.; Tanner, J. E. *J. Chem. Phys.* **1965**, *42*, 288.
20. Nuss, M. E.; James, T. L.; Apple, M. A.; Kollman, P. A. *Biochem. Biophys. Acta* **1980**, *609*, 136.
21. Barthwal, R.; Srivastava, N.; Sharma, U.; Govil, G. *J. Mol. Struct.* **1994**, *327*, 201.
22. Barthwal, R.; Mujeeb, A.; Srivastava, N.; Sharma, U. *Chem.-Biol. Interact.* **1996**, *100*, 125.
23. Barthwal, R.; Jain, M.; Awasthi, P.; Srivastava, N.; Sharma, U.; Kaur, M.; Govil, G. *J. Biomol. Struct. Dyn.* **2003**, *21*, 407.
24. Barthwal, R.; Awasthi, P.; Monica; Kaur, M.; Sharma, U.; Srivastava, N.; Barthwal, S. K.; Govil, G. *J. Struct. Biol.* **2004**, *148*, 34.
25. Wüthrich, K. In *NMR of Proteins and Nucleic Acids*; Wiley Interscience: New York, 1986.
26. Qu, X.; Wan, C.; Becker, H.; Zhong, D.; Zewail, A. H. *Proc. Natl. Acad. Sci. U.S.A.* **2001**, *98*, 14212.
27. Johnson, I. M.; kumar, S. G. B.; Malathi, R. *J. Biomol. Struct. Dyn.* **2003**, *20*, 677.
28. Lavery, R.; Sklenar, H. CURVES *5.1. Helical Analysis of Irregular Nucleic Acids*; Laboratory of Theoretical Biology, CNRS: Paris, 1996.
29. Lavery, R.; Sklenar, H. *J. Biomol. Struct. Dyn.* **1989**, *6*, 655.
30. Wang, A. H. J.; Ughetto, G.; Quigley, G. J.; Rich, A. *Biochemistry* **1987**, *26*, 1152.
31. Moore, M. H.; Hunter, W. N.; d'Estaintot, L.; Kennard, O. *J. Mol. Biol.* **1989**, *206*, 693.
32. Williams, L. D.; Frederick, C. A.; Ughetto, G.; Rich, A. *Nucleic Acids Res.* **1990**, *18*, 5533.
33. Neidle, S.; Taylor, G. *Biochim. Biophys. Acta* **1977**, *478*, 450.
34. Chaires, J. B.; Dattagupta, N.; Crothers, D. M. *Biochemistry* **1982**, *21*, 3933.
35. Von Dreele, R. B.; Einck, J. J. *Acta Crystallogr., Sect. B* **1977**, *33*, 3283.
36. Anguilli, R.; Foresti, E.; Rivi di, S. L.; Issacs, N. W.; Kennard, O.; Motherwell, W. D. S.; Wampler, D. L.; Arcamone, F. *Nat. (London) New Biol.* **1971**, *234*, 78.
37. Courseille, C.; Busetta, B.; Geoffre, S.; Hospital, M. *Acta Crystallogr., Sect. B* **1979**, *35*, 764.

38. Lipscomb, L. A.; Peek, M. E.; Zhou, F. X.; Berrand, J. A.; Van Derveer, D.; Williams, L. D. *Biochemistry* **1994**, *33*, 3649.
39. Podell, E. R.; Harrigton, D. J.; Taatzes, D. J.; Koch, T. H. *Acta Crystallogr., Sect. D* **1999**, *55*, 1516.
40. Taatzes, D. J.; Fenick, D. J.; Koch, T. H. *Chem. Res. Toxicol.* **1999**, *12*, 588.
41. Pan, S.; Bachur, N. R. *Mol. Pharmacol.* **1980**, *17*, 95.
42. Kleyer, D. L.; Koch, T. H. *J. Am. Chem. Soc.* **1983**, *105*, 2504.
43. Malatesta, V.; Penco, S.; Sacchi, N.; Valentini, L.; Vigevani, A.; Arcamone, F. *Can. J. Chem.* **1984**, *62*, 2845.
44. Agrawal, P.; Barthwal, S. K.; Barthwal, R. *European Journal of Medicinal Chemistry* **2008**. doi:10.1016/j.ejmech.2008.09.037.